Modelling Magnetic Confinement in Two-Dimensional Quantum Dots via Gauge-Invariant Imaginary-Time Propagation

Urvi Mukherjee, Nikhil Yenugu, and Sangita Sen*

Indian Institute of Science Education and Research (IISER) Kolkata, Department of Chemical Sciences, Mohanpur, West Bengal, 741246, India

E-mail: sangita.sen@iiserkol.ac.in

Contents

Pedagogical Derivation of the Wilson Hamiltonian in Symmetric Gauge

We aim to derive a discrete lattice Hamiltonian for a single charged particle moving in two dimensions under a magnetic field. The continuous Hamiltonian in the presence of a vector potential $\mathbf{A}(\mathbf{r})$ is:

$$\hat{H} = \frac{1}{2m} \left(\hat{\mathbf{p}} - q\mathbf{A}(\mathbf{r})\right)^2 + V(\mathbf{r})$$

where: m is the particle mass, q is the electric charge of the particle, $\hat{\mathbf{p}} = -i\hbar\nabla$ is the momentum operator, $\mathbf{A}(\mathbf{r})$ is the vector potential, $V(\mathbf{r})$ is an external scalar potential.

Our goal is to obtain a gauge-invariant lattice version of this Hamiltonian using the Wilson prescription, in particular leading to a discrete Hamiltonian that matches Eq. (7) of

the main manuscript. The space is discretized on a 2D square spatial lattice with uniform spacing Δx along the x-axis and Δy along the y-axis. The grid points are labeled by integers $x, y \in \mathbf{Z}$, corresponding to physical positions:

$$\mathbf{r} = (x\Delta x, y\Delta y)$$

The wavefunction $\psi(x, y)$ is now defined on lattice sites (x, y).

The second derivative along x in the absence of a magnetic field is discretized as:

$$\frac{\partial^2 \psi}{\partial x^2} \approx \frac{1}{(\Delta x)^2} \left[\psi(x+1, y) - 2\psi(x, y) + \psi(x-1, y)\right]$$

This is the standard finite-difference discretization of the Laplacian. In the presence of a magnetic field, however, this form is not gauge-invariant.

To maintain gauge invariance in a magnetic field, we replace ordinary finite differences with gauge-covariant differences using Wilson line factors (also known as Peierls substitution):

$$U_x(x, y) = \exp\left[\frac{iq\Delta x}{\hbar} A_x(x, y)\right]$$
$$U_y(x, y) = \exp\left[\frac{iq\Delta y}{\hbar} A_y(x, y)\right]$$

These link variables transport the wavefunction from neighboring sites with the phase accumulated due to the vector potential.

The covariant second derivative along x-direction is:

$$D_x^2 \psi(x, y) = \frac{1}{(\Delta x)^2} \left[2\psi(x, y) - U_x(x, y)\psi(x+1, y) - U_x^\dagger(x-1, y)\psi(x-1, y)\right]$$

Likewise, the covariant second derivative along y-direction is:

$$D_y^2\psi(x,y) = \frac{1}{(\Delta y)^2}\left[2\psi(x,y) - U_y(x,y)\psi(x,y+1) - U_y^\dagger(x,y-1)\psi(x,y-1)\right]$$

The full lattice Hamiltonian (Wilson Hamiltonian) is:

$$(\hat{H}_{\mathrm{WH}}\psi)(x,y) = -\frac{\hbar^2}{2m}\left(D_x^2\psi(x,y) + D_y^2\psi(x,y)\right) + V(x,y)\psi(x,y)$$

Substituting the discrete expressions of D_x^2 and D_y^2, we obtain:

$$\begin{aligned}(\hat{H}_{\mathrm{WH}}\psi)(x,y) = \frac{\hbar^2}{2m}\Bigg[&\frac{1}{(\Delta x)^2}\left(2\psi(x,y) - U_x(x,y)\psi(x+1,y) - U_x^\dagger(x-1,y)\psi(x-1,y)\right)\\ &+ \frac{1}{(\Delta y)^2}\left(2\psi(x,y) - U_y(x,y)\psi(x,y+1) - U_y^\dagger(x,y-1)\psi(x,y-1)\right)\Bigg]\\ &+ V(x,y)\psi(x,y)\end{aligned}$$

This expression is Hermitian and gauge invariant.

We now compute the matrix elements of the Hamiltonian operator $\hat{H}_{\mathrm{WH}}$ in the lattice position basis. Let us denote:

$$H_{x_1,y_1;x_2,y_2} = \langle x_1, y_1|\hat{H}_{\mathrm{WH}}|x_2, y_2\rangle$$

Using the discrete form from Section 6, we obtain nonzero contributions to $H_{x_1,y_1;x_2,y_2}$ only for sites that are the same or nearest neighbors:

$$\begin{aligned}H_{x_1,y_1;x_2,y_2} = &\left[\frac{\hbar^2}{2m}\left(\frac{2}{(\Delta x)^2} + \frac{2}{(\Delta y)^2}\right) + V(x_1,y_1)\right]\delta_{x_1,x_2}\delta_{y_1,y_2}\\ &- \frac{\hbar^2}{2m(\Delta x)^2}\left[U_x(x_1,y_1)\delta_{x_1+1,x_2} + U_x^\dagger(x_2,y_2)\delta_{x_1-1,x_2}\right]\delta_{y_1,y_2}\\ &- \frac{\hbar^2}{2m(\Delta y)^2}\left[U_y(x_1,y_1)\delta_{y_1+1,y_2} + U_y^\dagger(x_2,y_2)\delta_{y_1-1,y_2}\right]\delta_{x_1,x_2}\end{aligned}$$

This matrix element clearly connects to the earlier expression of the action of $\hat{H}_{\mathrm{WH}}$ on $\psi(x, y)$, and provides the link to the full Hamiltonian matrix used for diagonalization.

1 Wavefunctions of 2D Harmonic Oscillator system

The probability density, real and imaginary parts of the first six numerically obtained (on a 240 nm x 240 nm grid, with 65 x 65 grid points) eigenfunctions of the system of a single electron (charge $q = -e$, where e is the elementary charge) in GaAs (effective mass $m = 0.067m_e$, where m_e is the rest mass of the electron), in a confining potential of $\hbar\omega_0 = 4$ meV, varying magnetic field strength (B (T) = 0, 1, 2, 3, 4, 5) is calculated.

1.1 Analytic

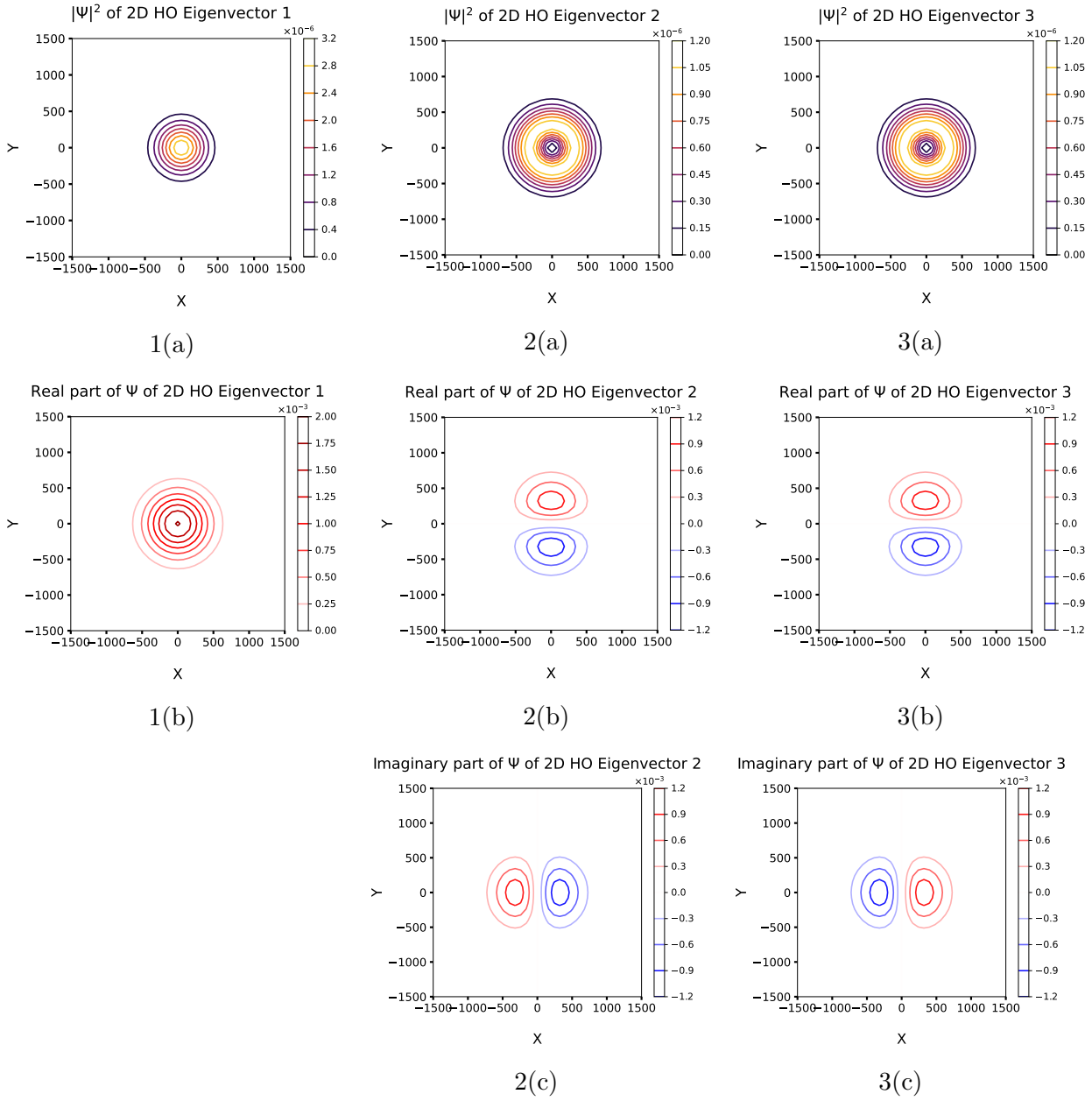

Figure 1: The (a) probability density, (b) real component and (c) phase of the analytical wavefunctions calculated using the ITEM at 65 grid points, in the absence of a uniform perpendicular magnetic field. The quantum numbers (n, M) of the eigenvectors are: 1. (0, 0), 2. (0, -1), 3. (0, 1).

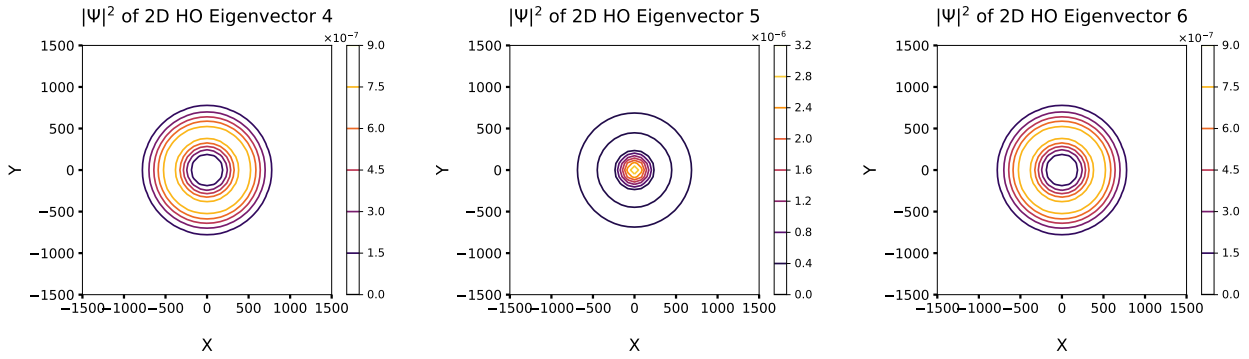

4(a) 5(a) 6(a)

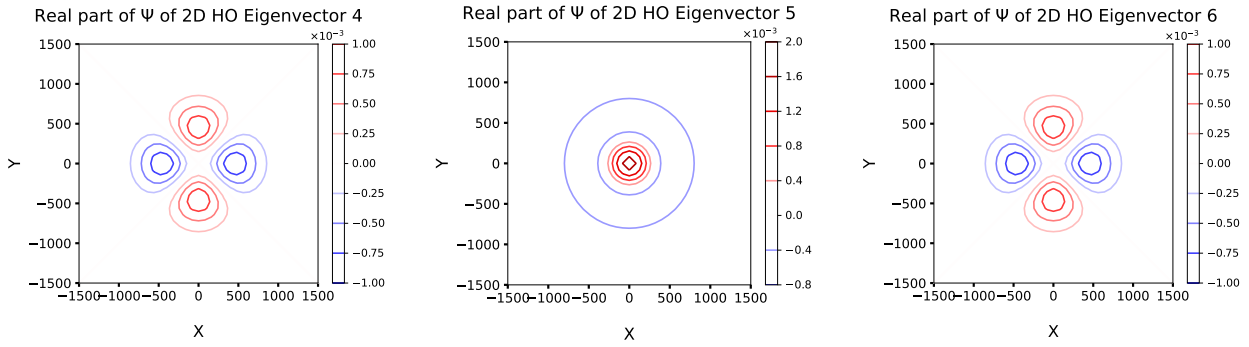

4(b) 5(b) 6(b)

4(c) 6(c)

Figure 2: The (a) probability density, (b) real component and (c) phase of the analytical wavefunctions calculated using the ITEM at 65 grid points, in the absence of a uniform perpendicular magnetic field. The quantum numbers (n, M) of the eigenvectors are: 4. (0, -2), 5. (1, 0), 6. (0, -2)

1.2 Numerical

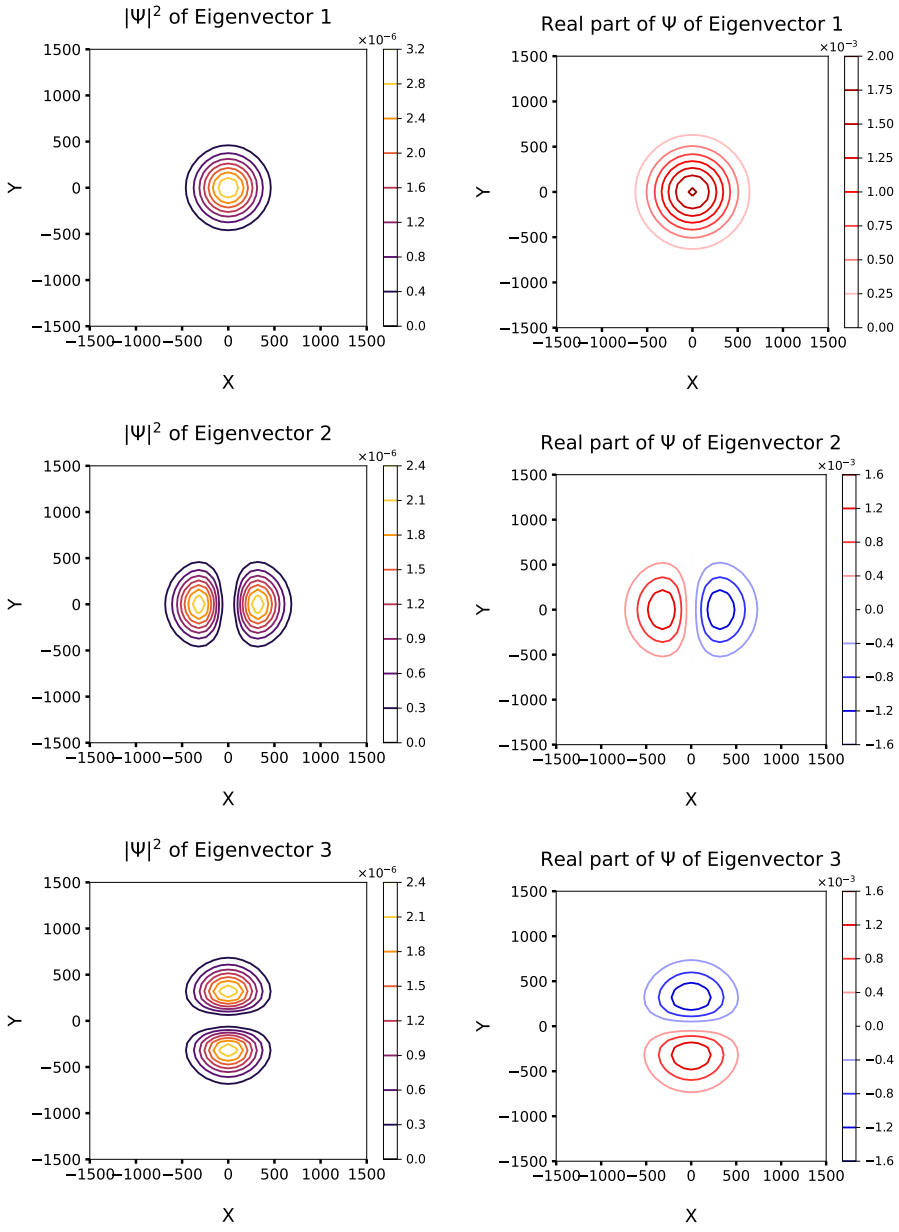

Figure 3: The probability density contour plots of the 1st, 2nd and 3rd numerically obtained eigenfunctions obtained using ITP for magnetic field strength B = 0 T.

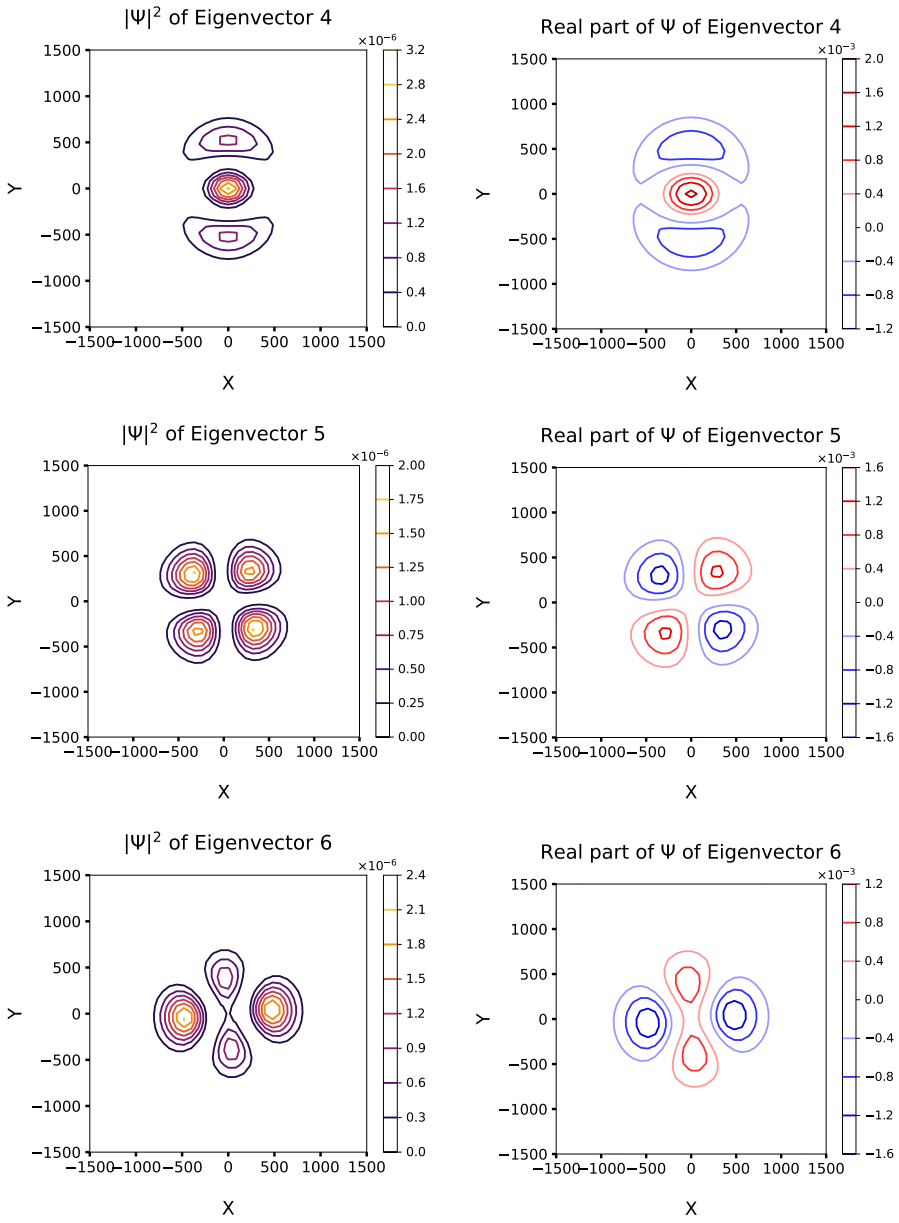

Figure 4: The probability density contour plots of the 4th, 5th and 6th numerically obtained eigenfunctions obtained using ITP for magnetic field strength B = 0 T.

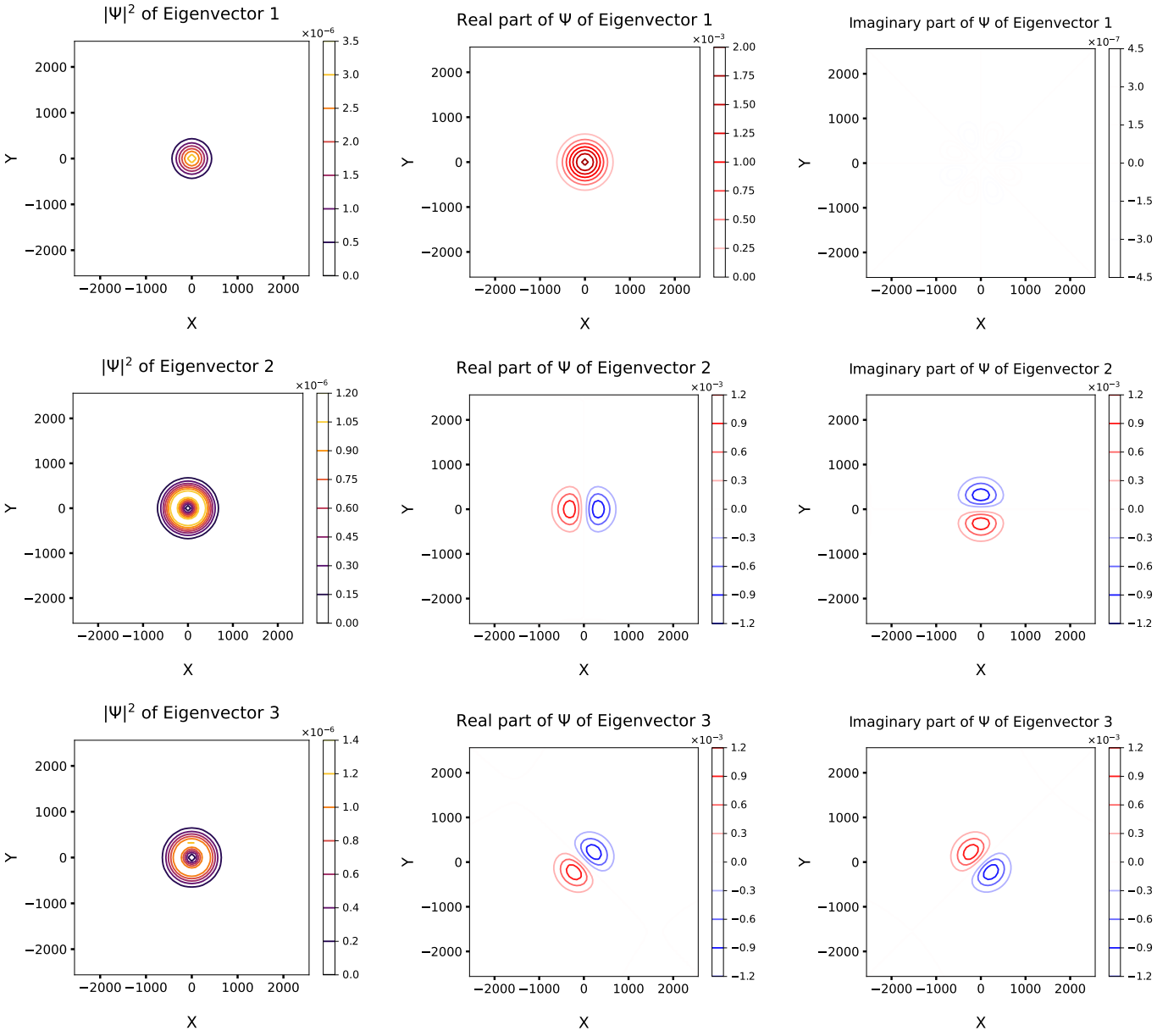

Figure 5: The probability density contour plots of the 1st, 2nd and 3rd numerically obtained eigenfunctions obtained using ITP for magnetic field strength B = 1 T.

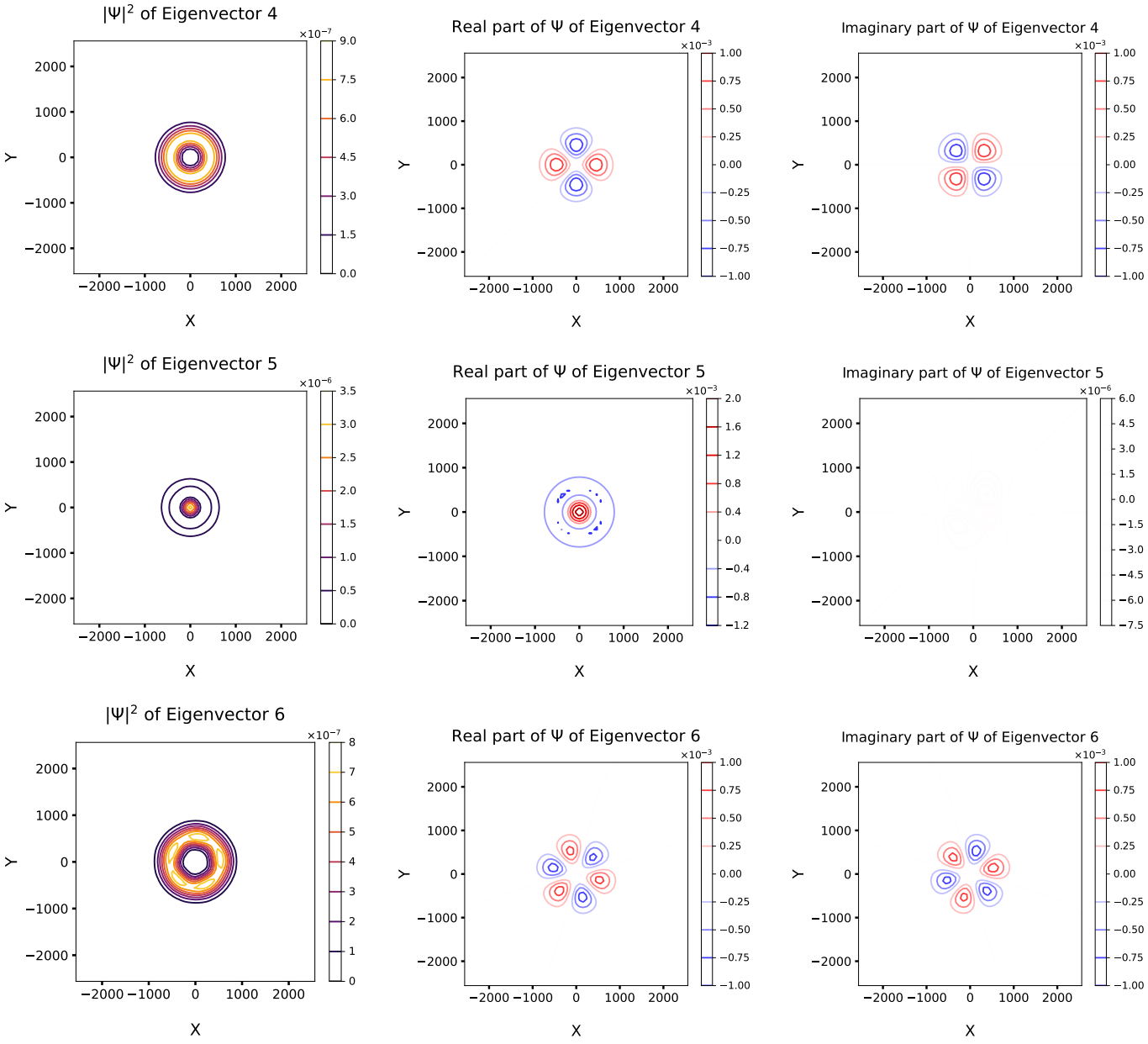

Figure 6: The probability density contour plots of the 4th, 5th and 6th numerically obtained eigenfunctions obtained using ITP for magnetic field strength B = 1 T.

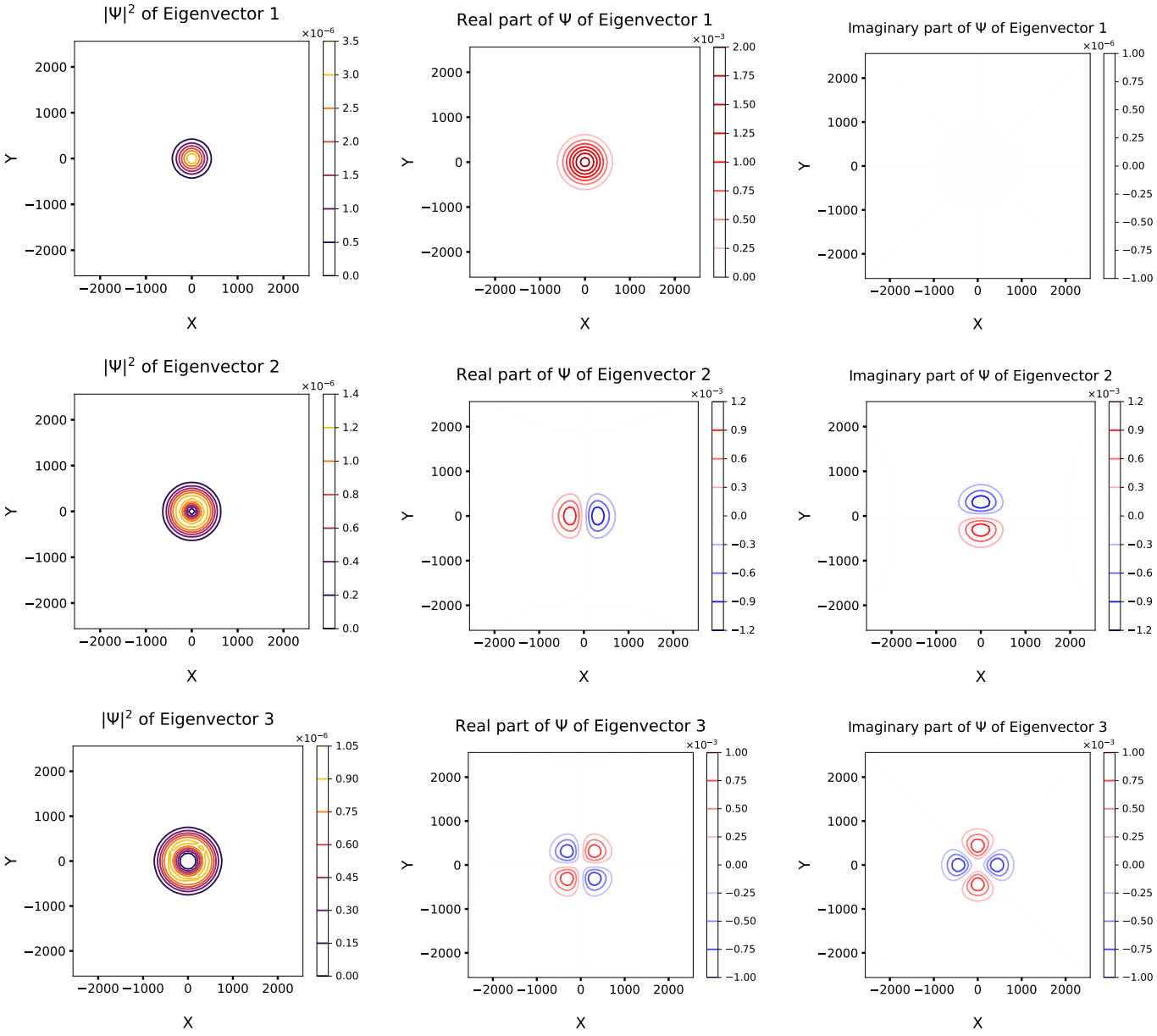

Figure 7: The probability density contour plots of the 1st, 2nd and 3rd numerically obtained eigenfunctions obtained using ITP for magnetic field strength B = 2 T.

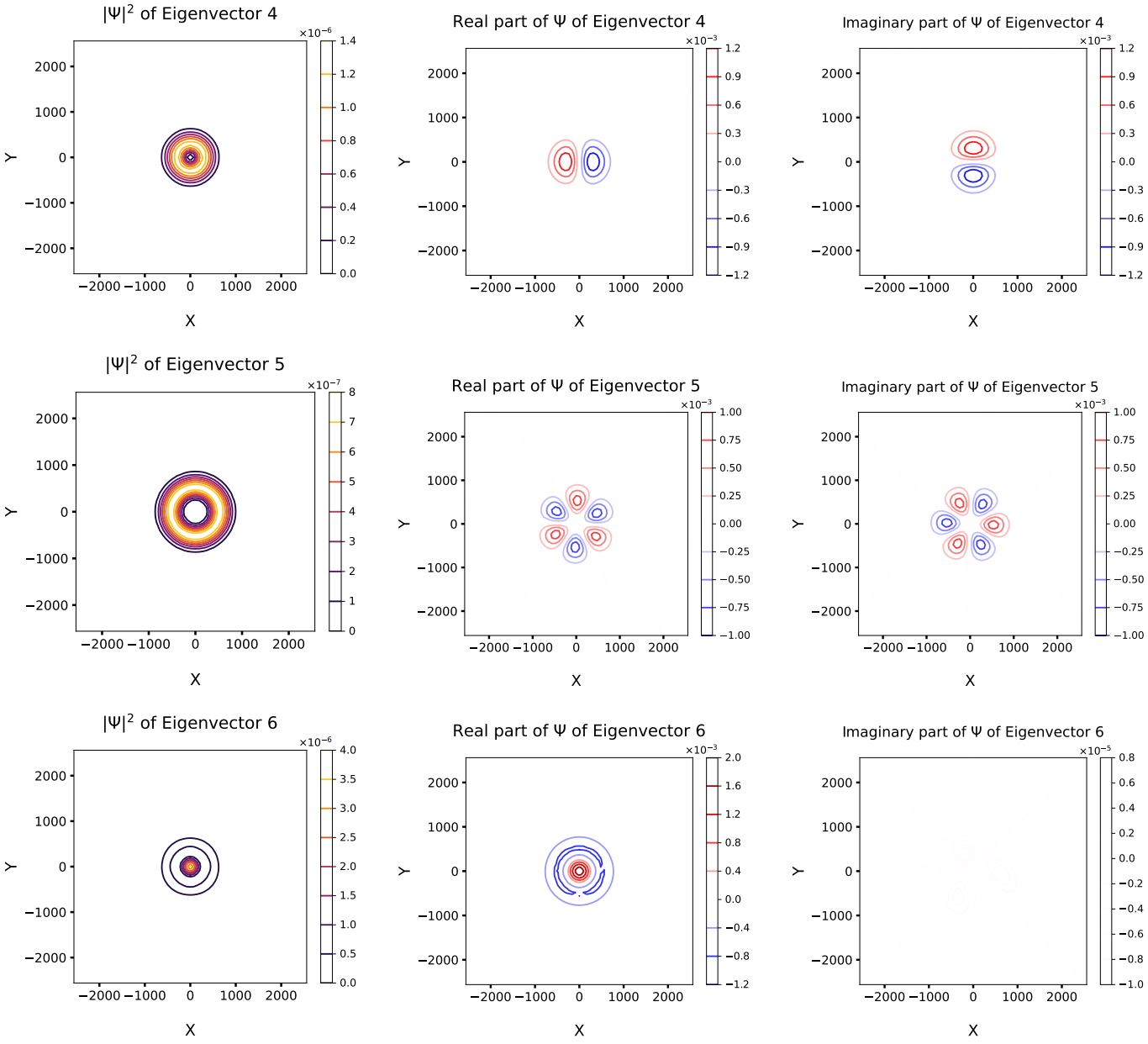

Figure 8: The probability density contour plots of the 4th, 5th and 6th numerically obtained eigenfunctions obtained using ITP for magnetic field strength B = 2 T.

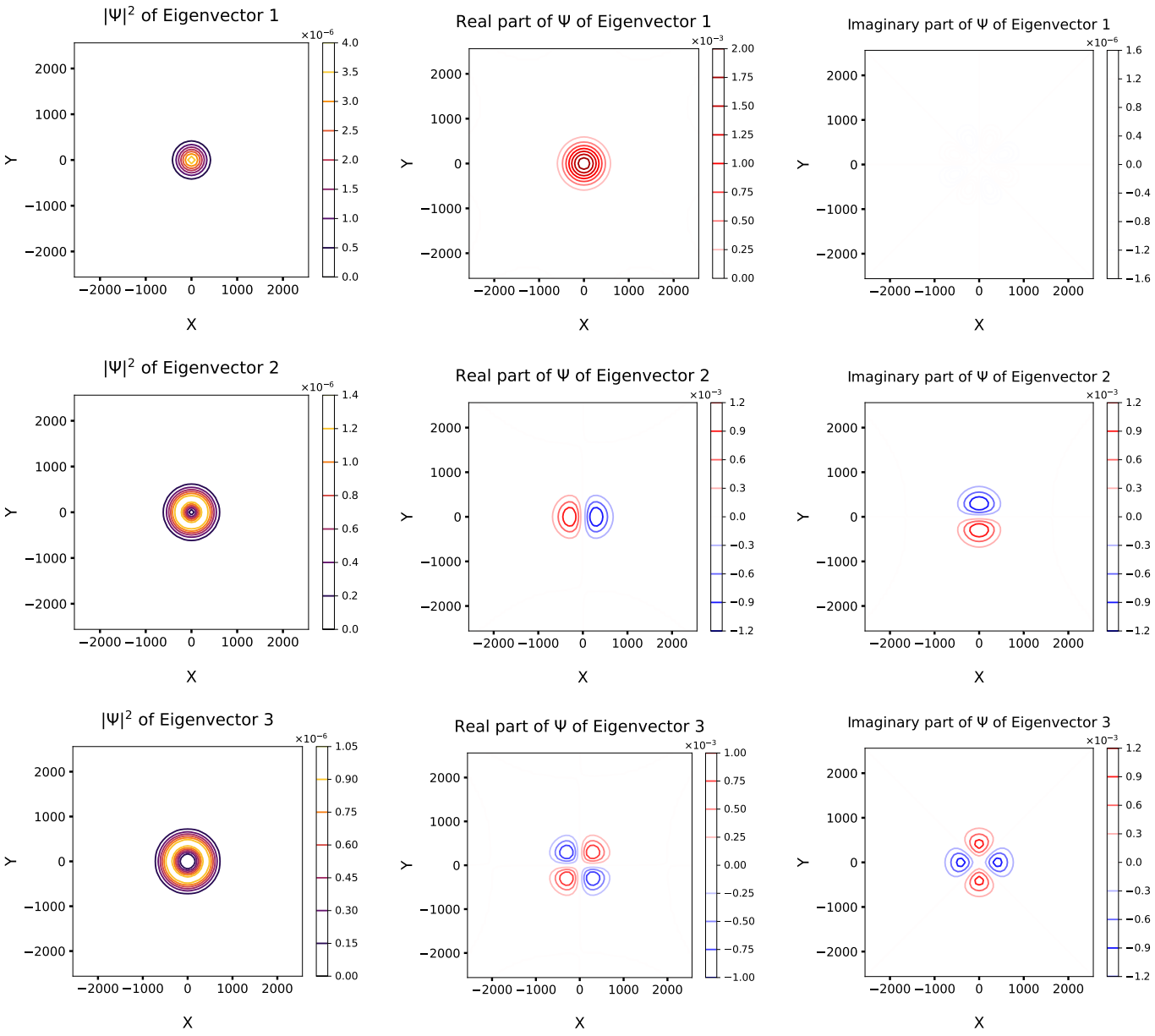

Figure 9: The probability density contour plots of the 1st, 2nd and 3rd numerically obtained eigenfunctions obtained using ITP for magnetic field strength B = 3 T.

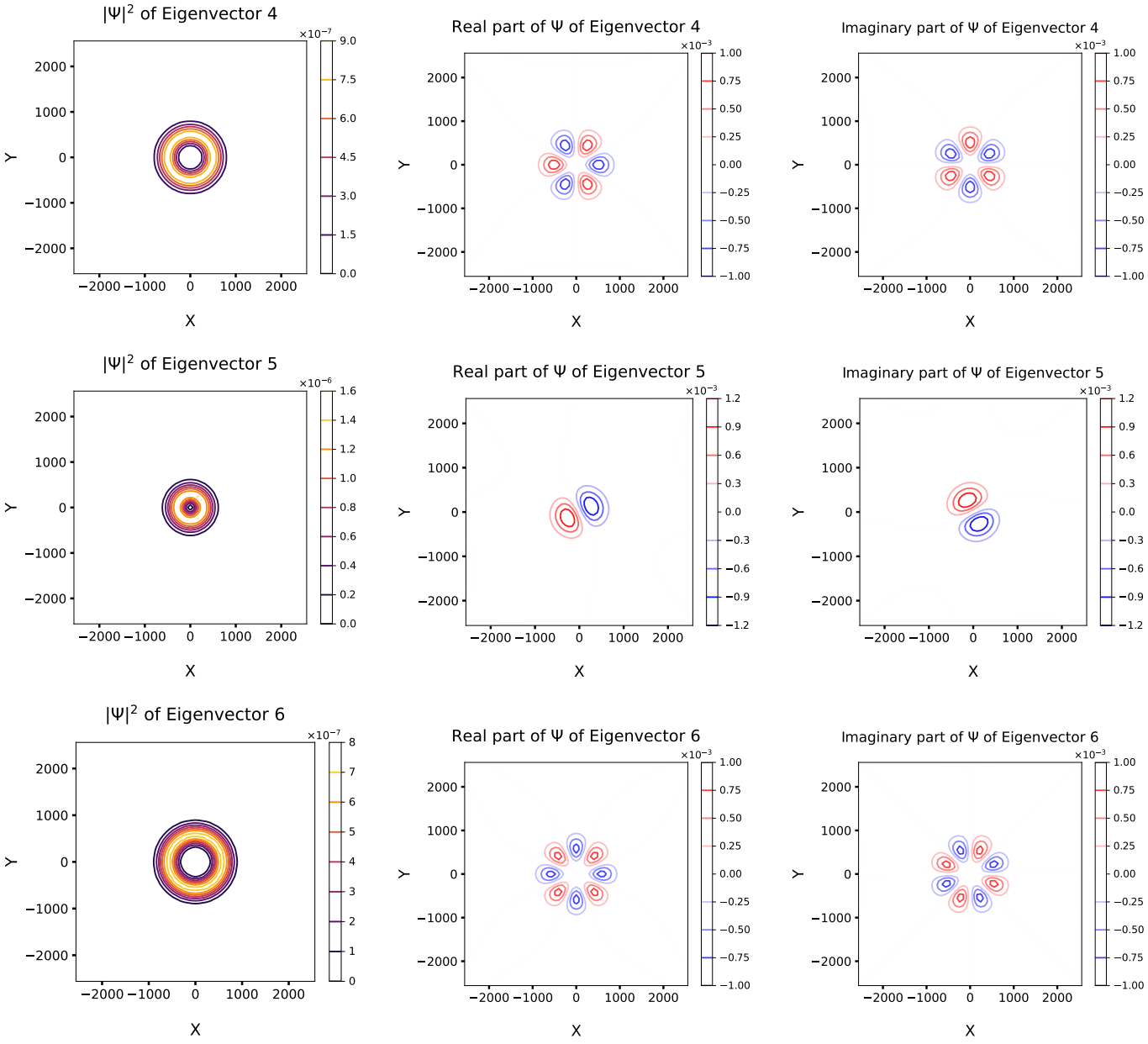

Figure 10: The probability density contour plots of the 4th, 5th and 6th numerically obtained eigenfunctions obtained using ITP for magnetic field strength B = 3 T.

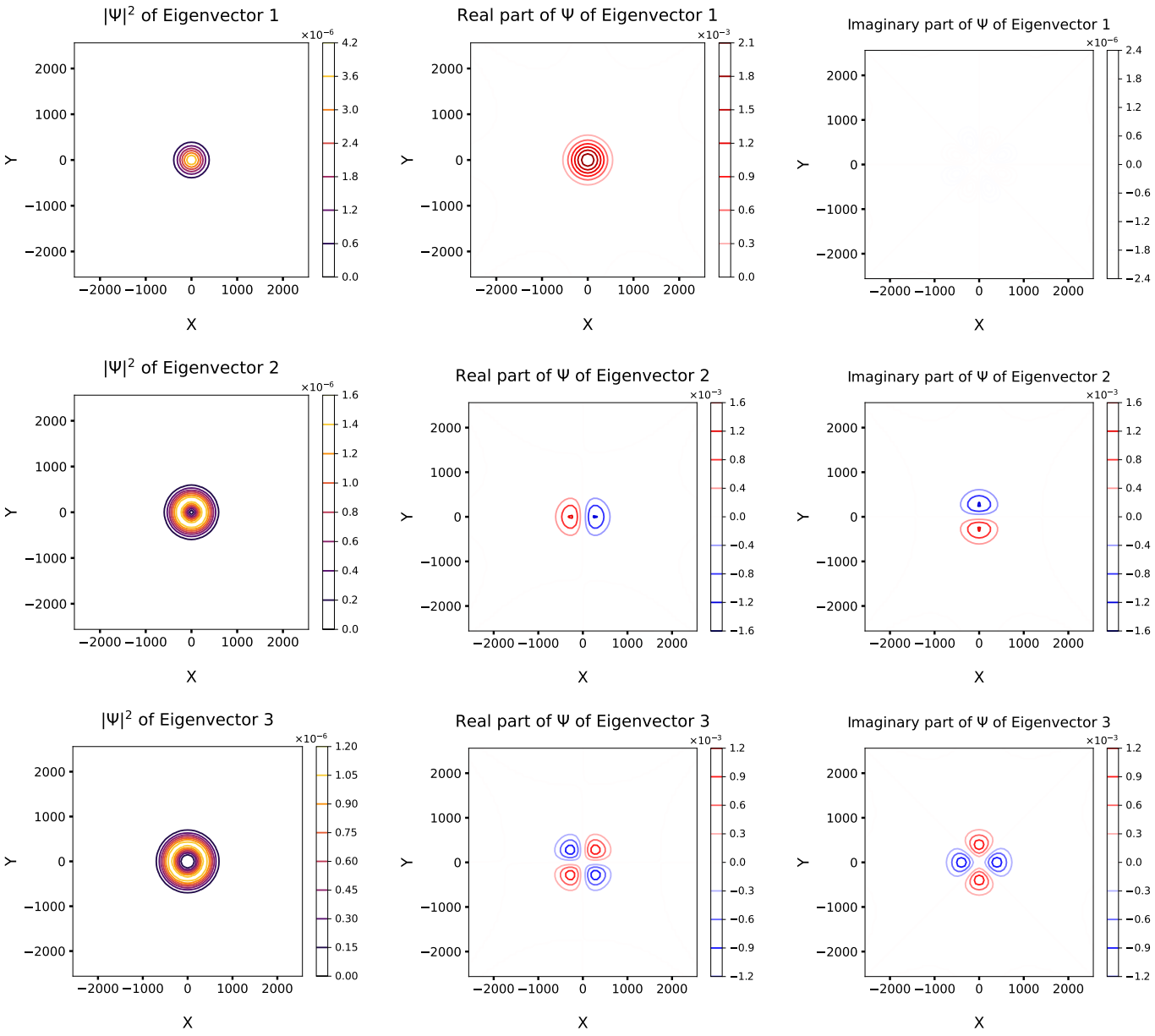

Figure 11: The probability density contour plots of the 1st, 2nd and 3rd numerically obtained eigenfunctions obtained using ITP for magnetic field strength B = 4 T.

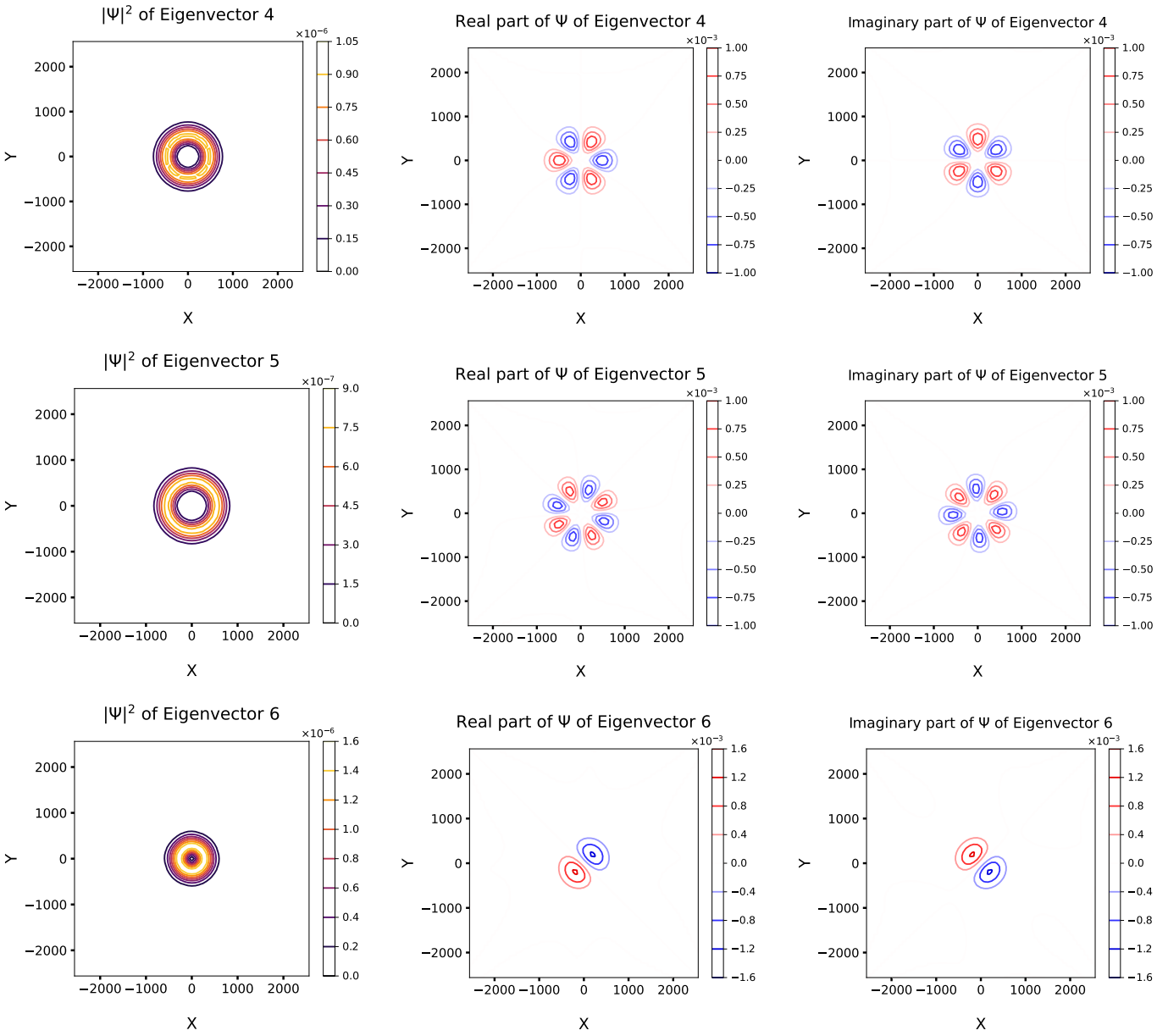

Figure 12: The probability density contour plots of the 4th, 5th and 6th numerically obtained eigenfunctions obtained using ITP for magnetic field strength B = 4 T.

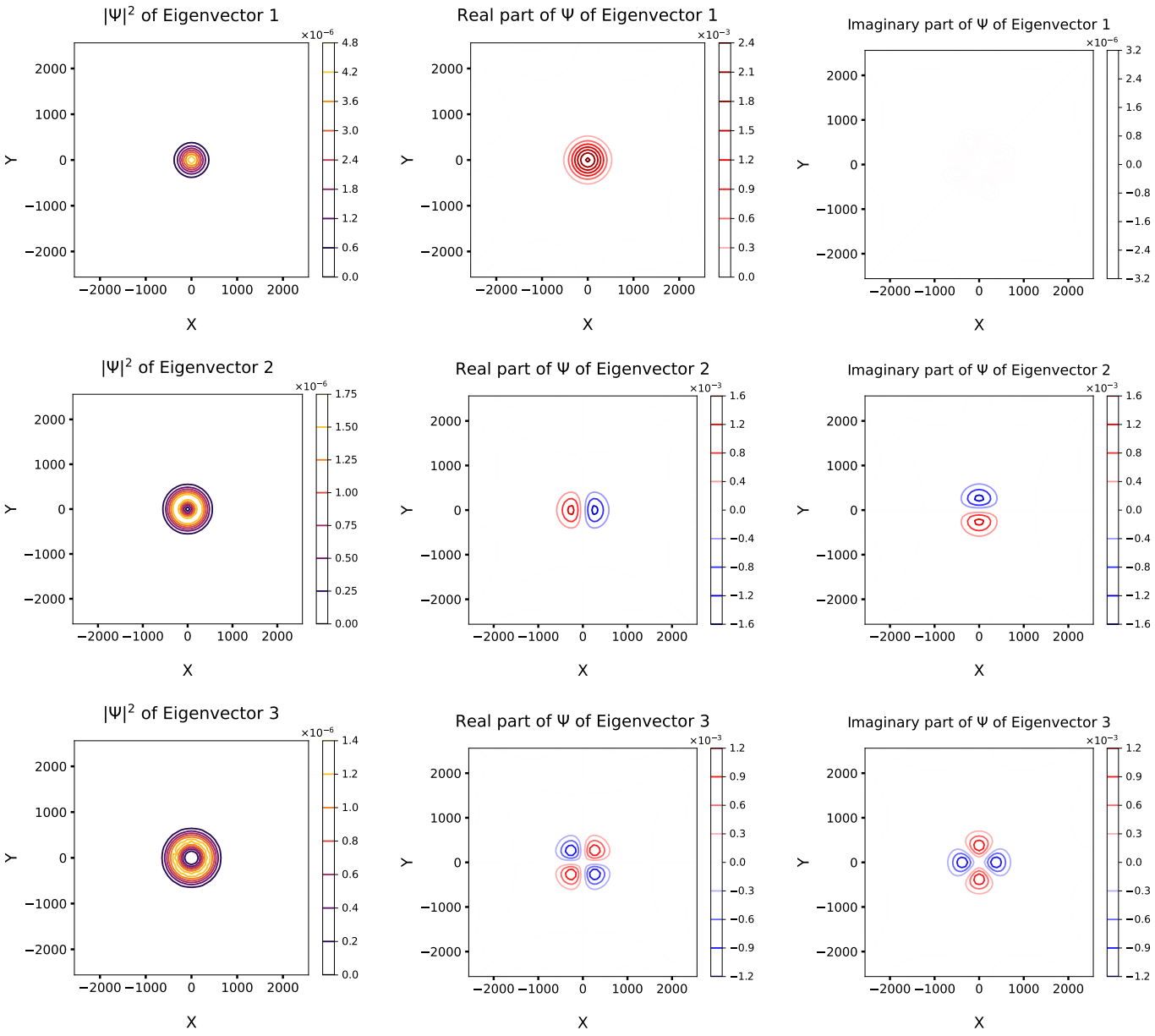

Figure 13: The probability density contour plots of the 1st, 2nd and 3rd numerically obtained eigenfunctions obtained using ITP for magnetic field strength B = 5 T.

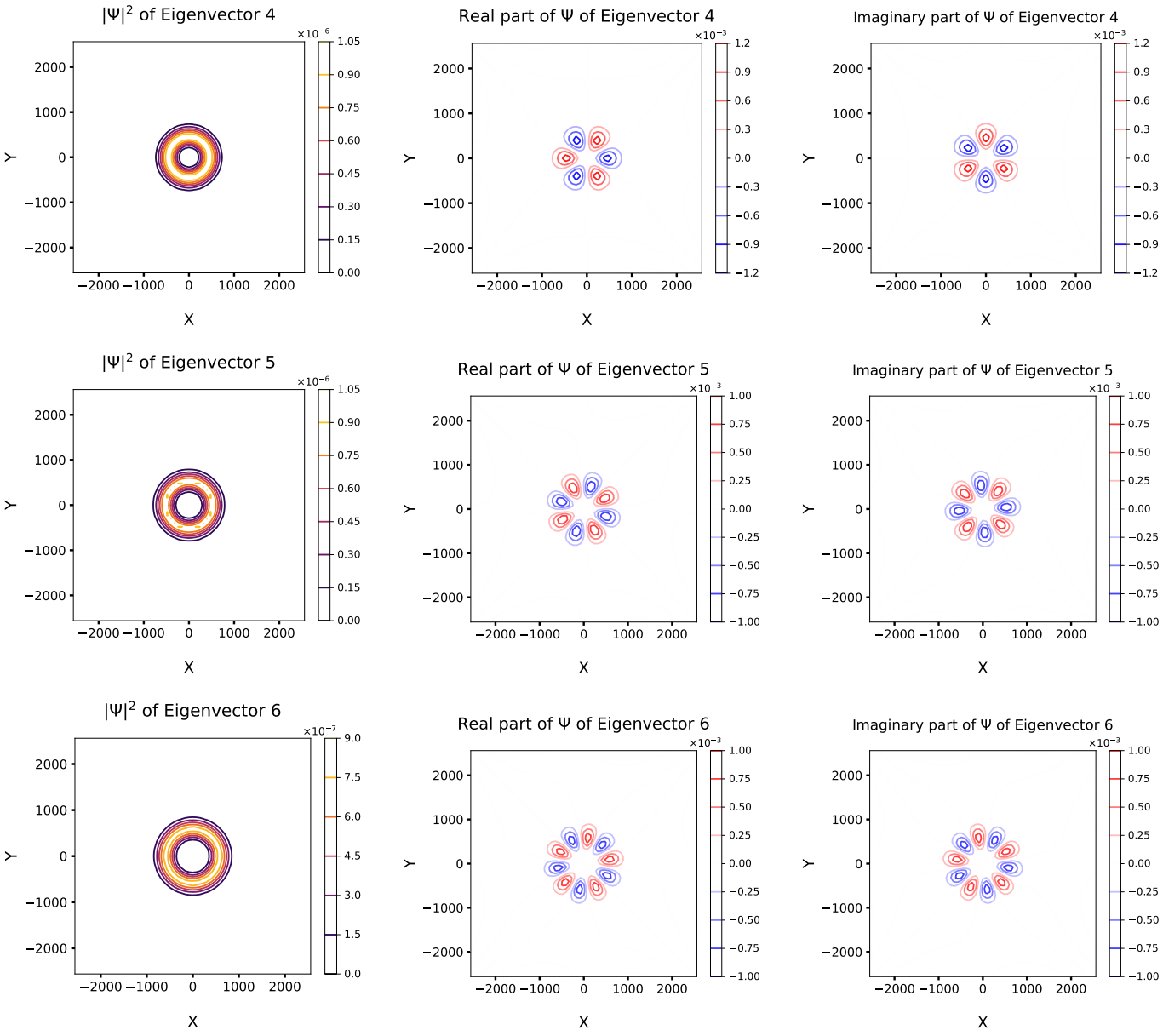

Figure 14: The probability density contour plots of the 4th, 5th and 6th numerically obtained eigenfunctions obtained using ITP for magnetic field strength B = 5 T.

2 Wavefunctions of the Gaussian system

We show the probability density, real and imaginary parts of the the numerically obtained (on a 121.7 nm x 121.7 nm, with 65 x 65 grid points) wavefunctions using the ITP for the system of a single electron ($q = -e$) in GaAs ($m = 0.067m_e$) in a Gaussian system with parameters $\alpha = 0.043$ nm^{-1} and $V_0 = 9.5$ meV, varying magnetic field strength (B (T) = 0, 1, 2, ..., 10):

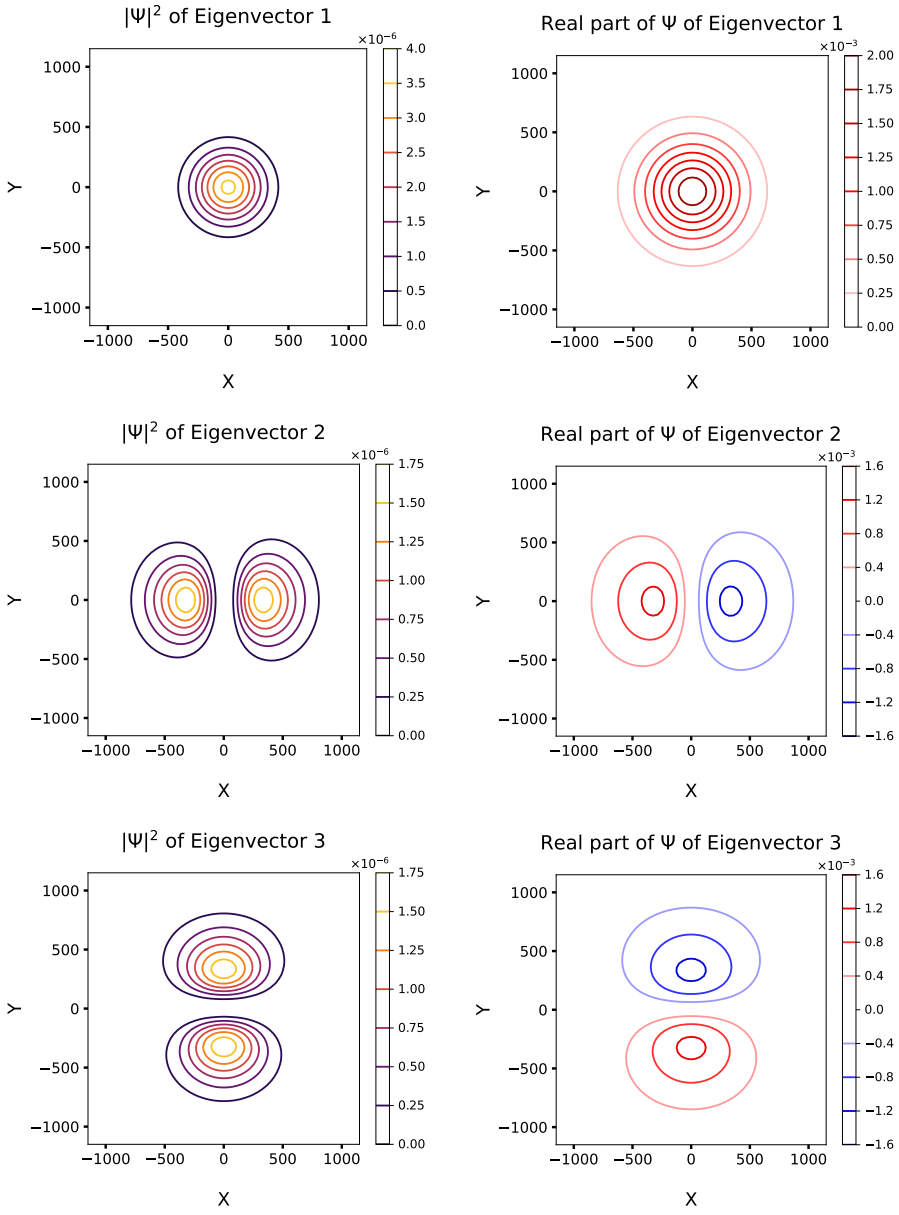

Figure 15: The probability density contour plots of the 1st, 2nd and 3rd numerically obtained eigenfunctions obtained using ITP for magnetic field strength B = 0 T.

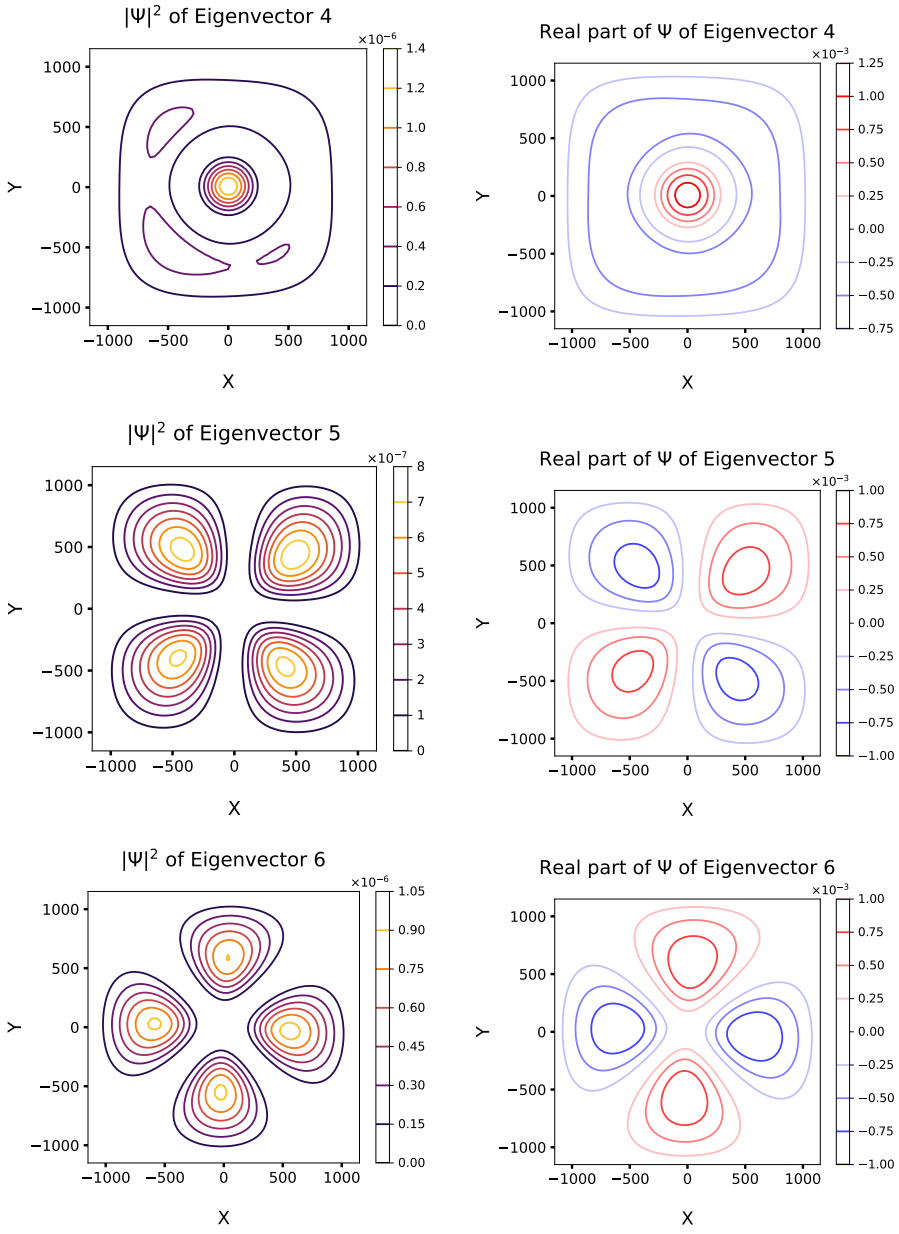

Figure 16: The probability density contour plots of the 4th, 5th and 6th numerically obtained eigenfunctions obtained using ITP for magnetic field strength B = 0 T.

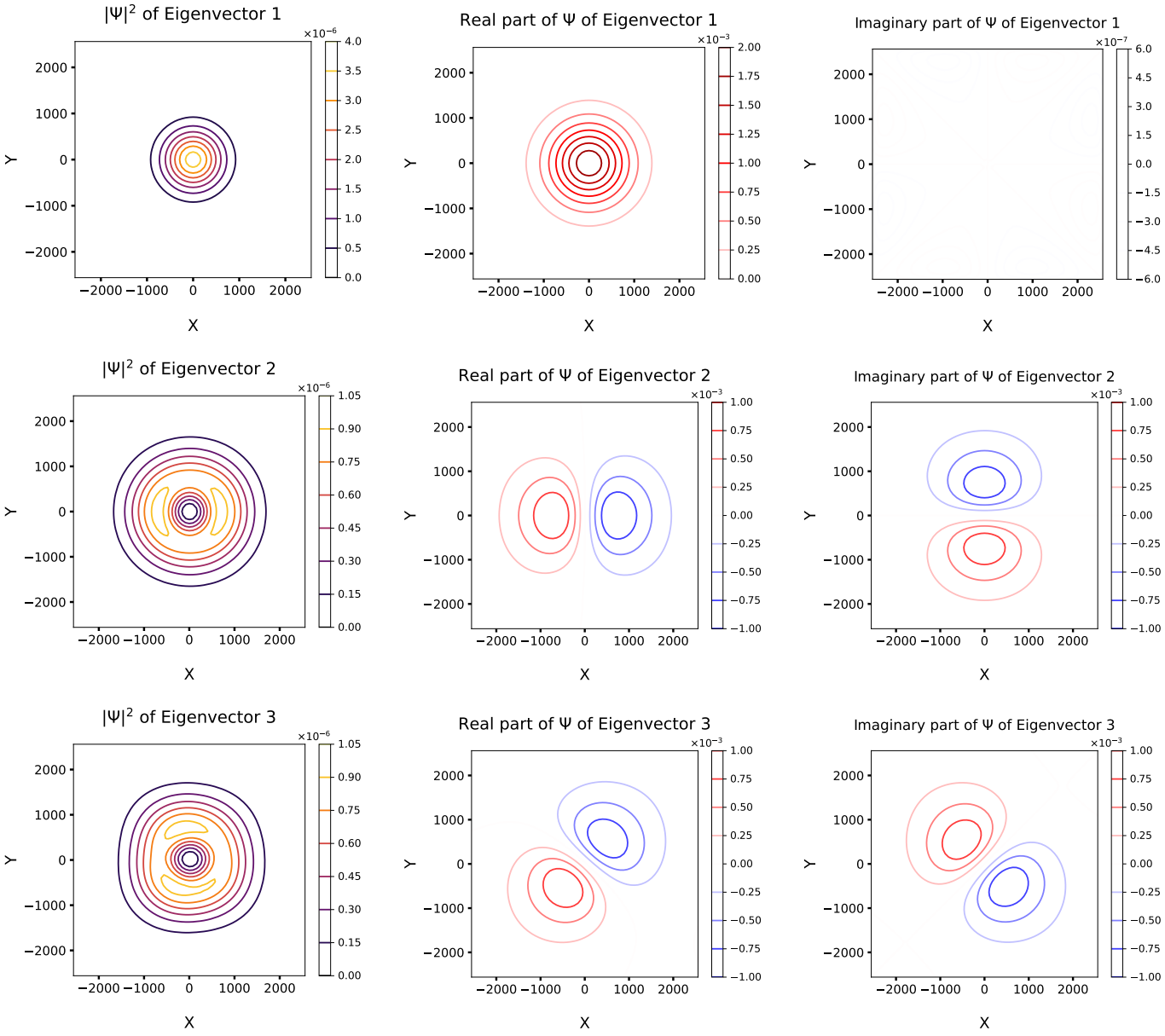

Figure 17: The probability density, real and imaginary contour plots of the 1st, 2nd and 3rd numerically obtained eigenfunctions obtained using ITP for magnetic field strength B = 1 T.

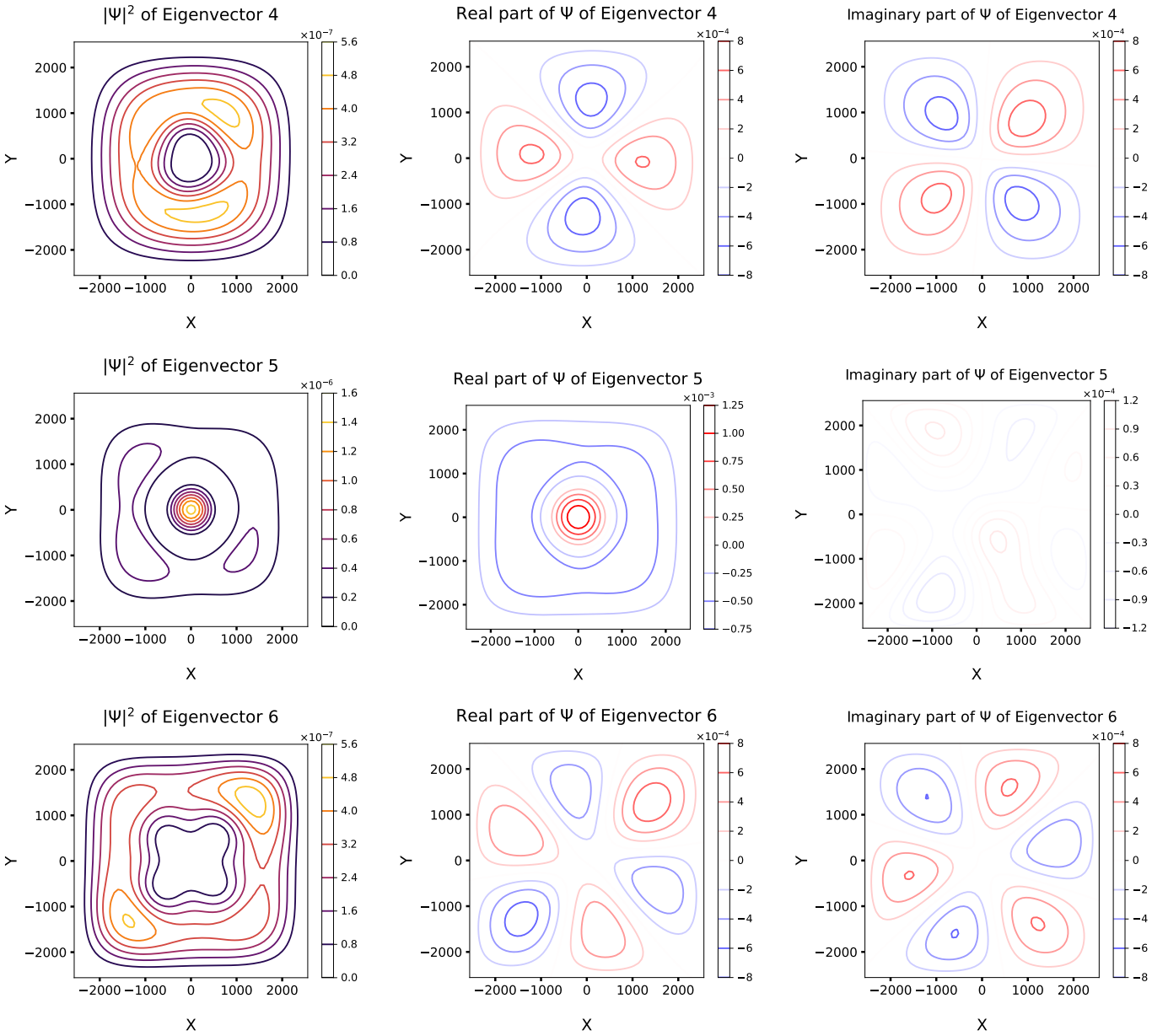

Figure 18: The probability density, real and imaginary contour plots of the 4th, 5th and 6th numerically obtained eigenfunctions obtained using ITP for magnetic field strength B = 1 T.

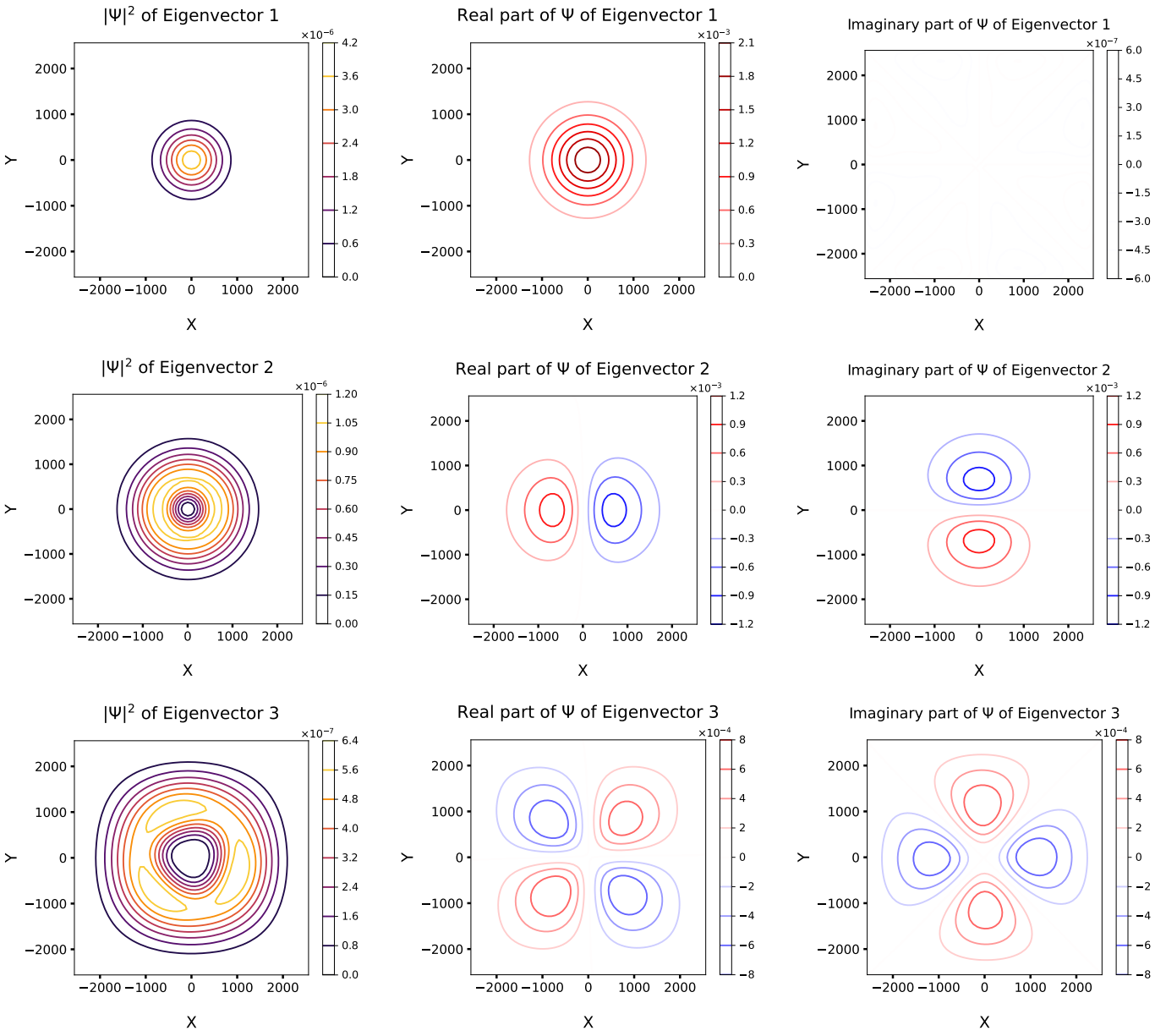

Figure 19: The probability density, real and imaginary contour plots of the 1st, 2nd and 3rd numerically obtained eigenfunctions obtained using ITP for magnetic field strength B = 2 T.

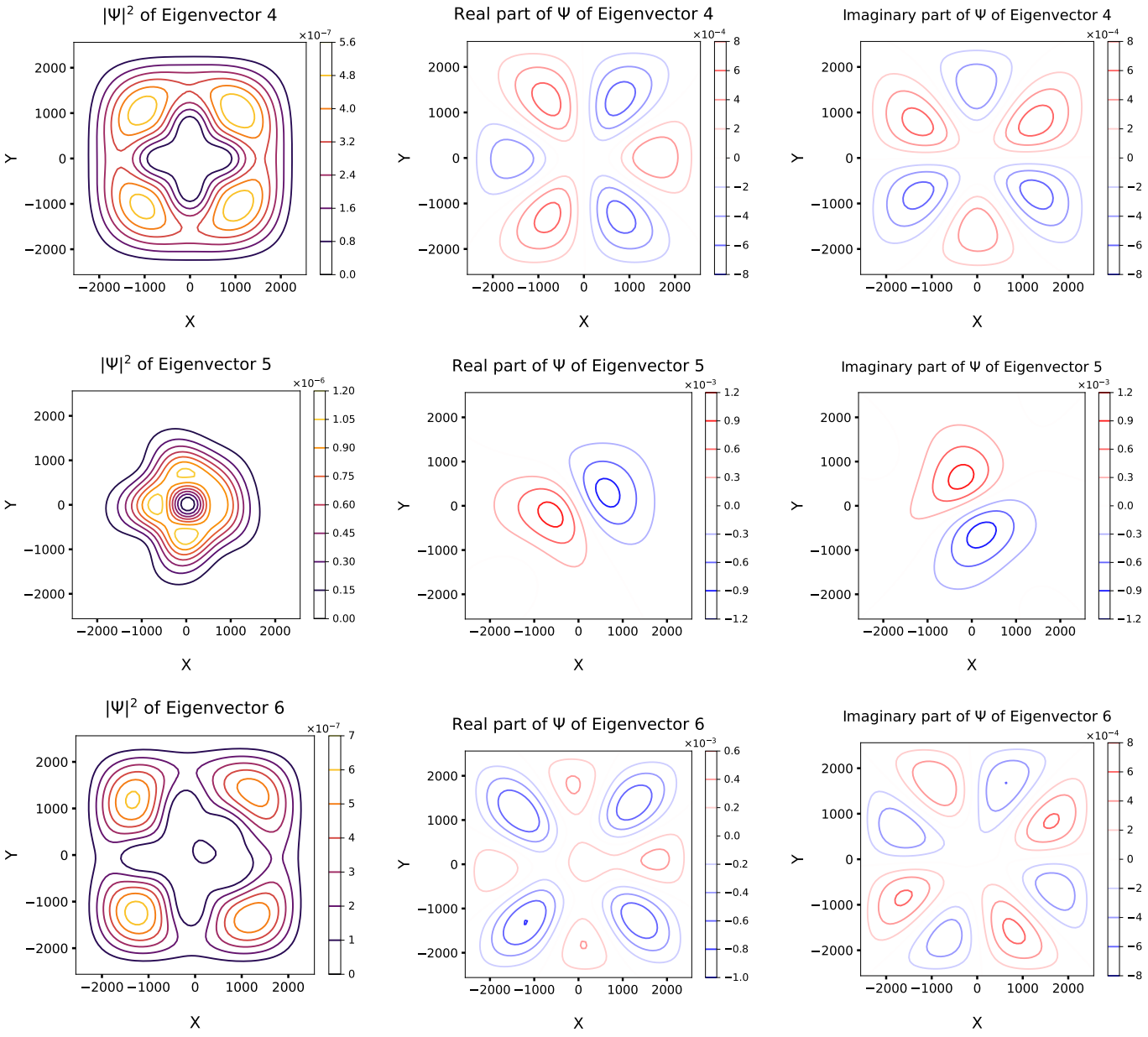

Figure 20: The probability density, real and imaginary contour plots of the 4th, 5th and 6th numerically obtained eigenfunctions obtained using ITP for magnetic field strength B = 2 T.

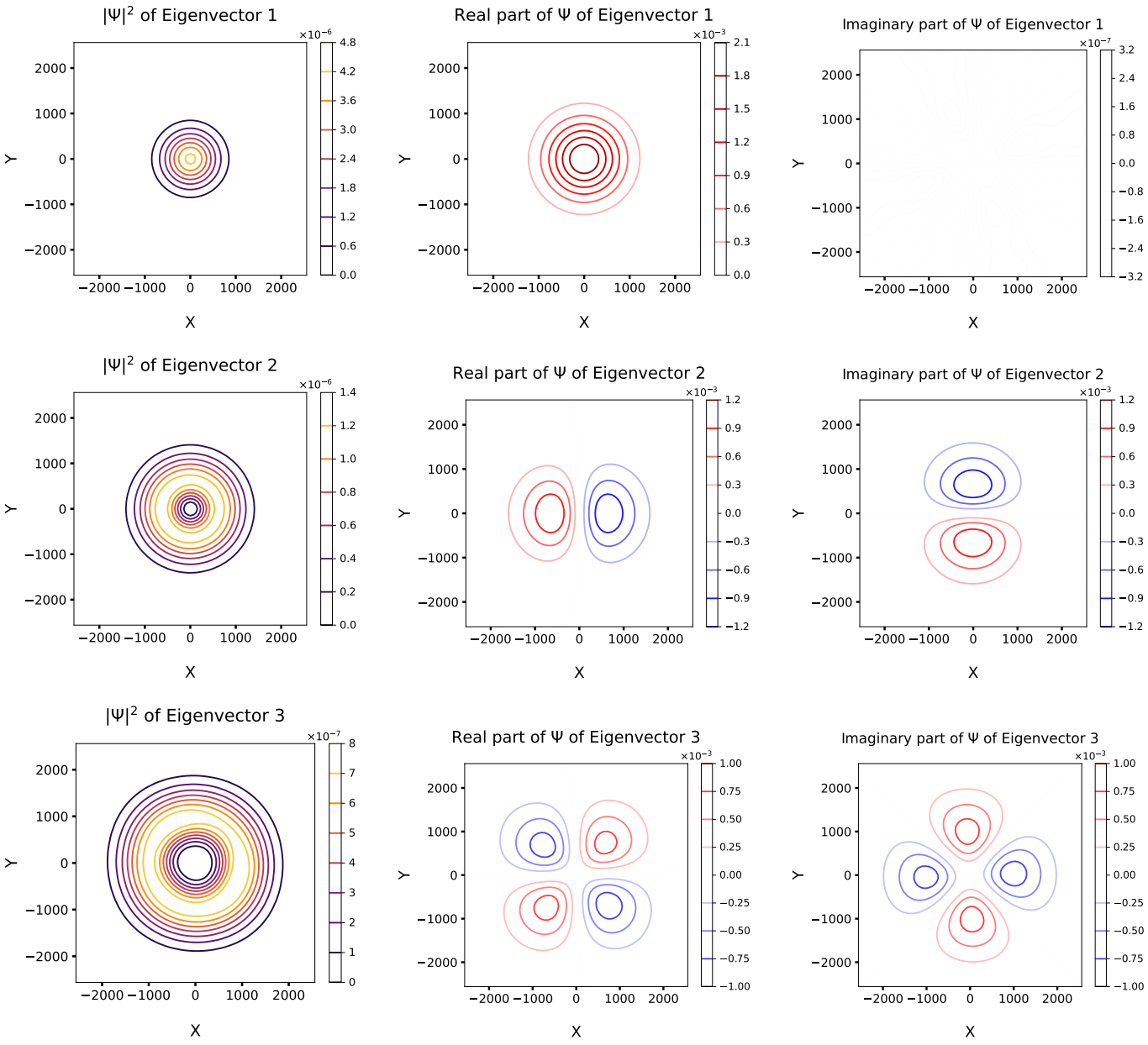

Figure 21: The probability density, real and imaginary contour plots of the 1st, 2nd and 3rd numerically obtained eigenfunctions obtained using ITP for magnetic field strength B = 3 T.

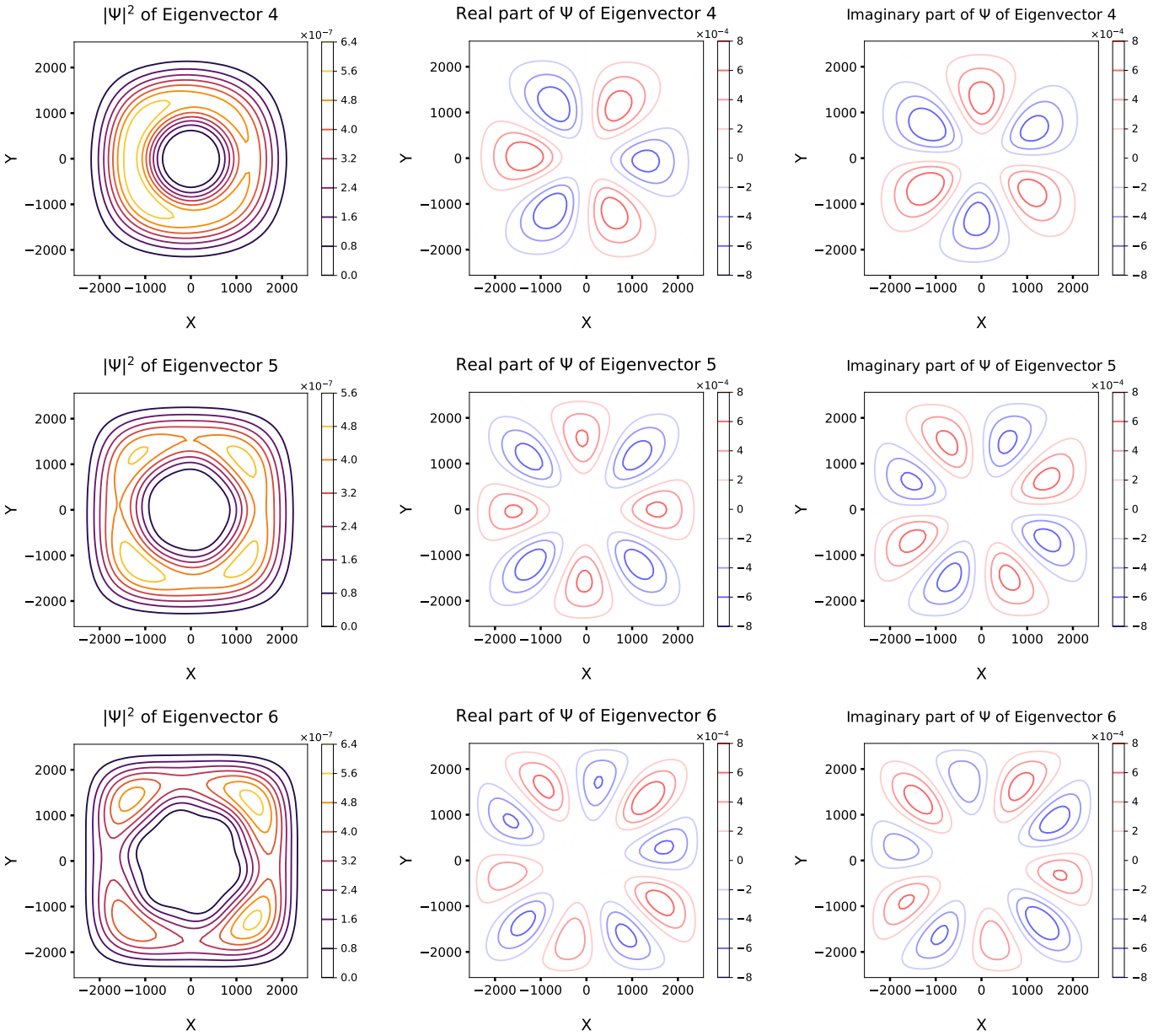

Figure 22: The probability density, real and imaginary contour plots of the 4th, 5th and 6th numerically obtained eigenfunctions obtained using ITP for magnetic field strength B = 3 T.

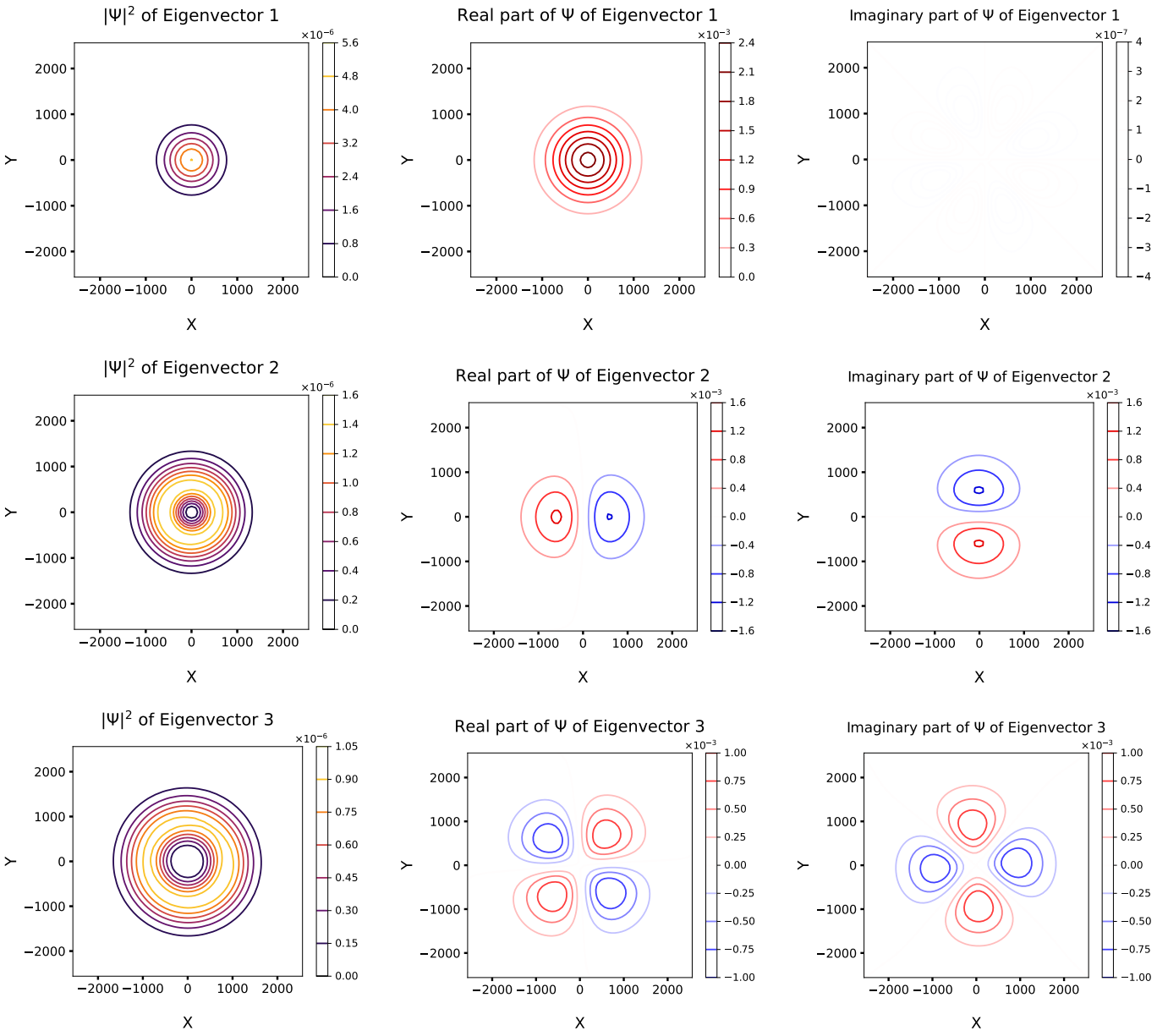

Figure 23: The probability density, real and imaginary contour plots of the 1st, 2nd and 3rd numerically obtained eigenfunctions obtained using ITP for magnetic field strength B = 4 T.

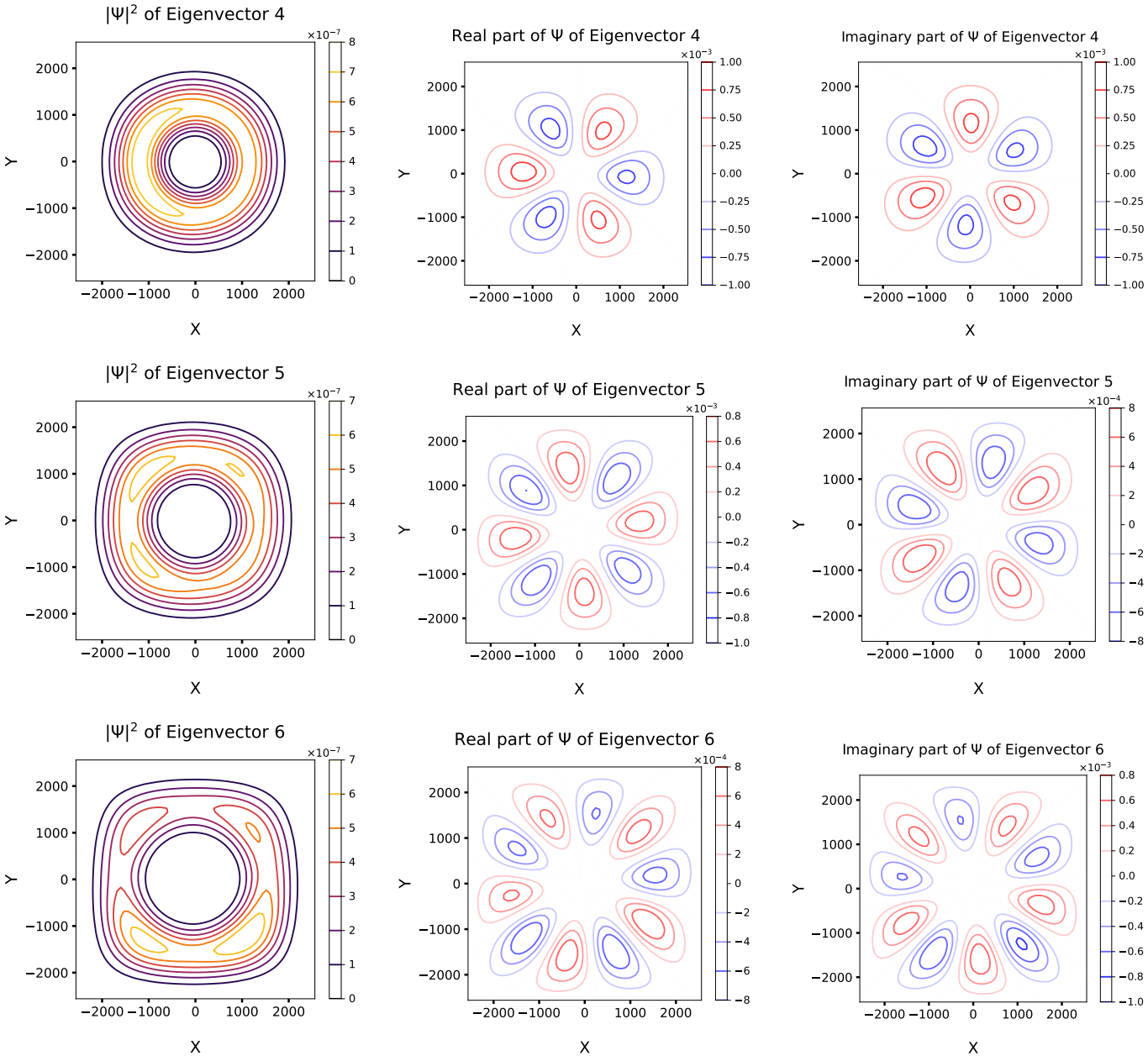

Figure 24: The probability density, real and imaginary contour plots of the 4th, 5th and 6th numerically obtained eigenfunctions obtained using ITP for magnetic field strength B = 4 T.

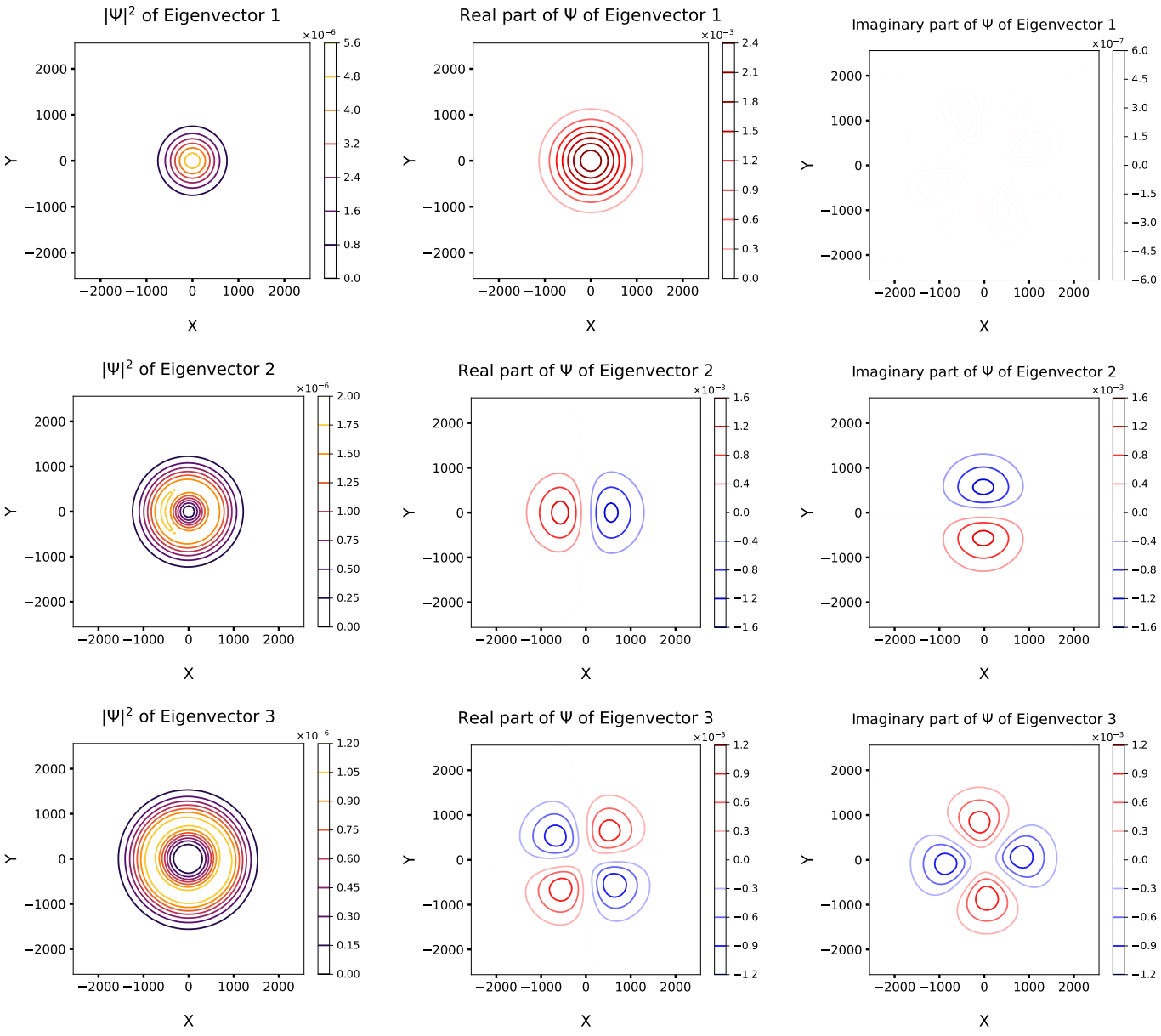

Figure 25: The probability density, real and imaginary contour plots of the 1st, 2nd and 3rd numerically obtained eigenfunctions obtained using ITP for magnetic field strength B = 5 T.

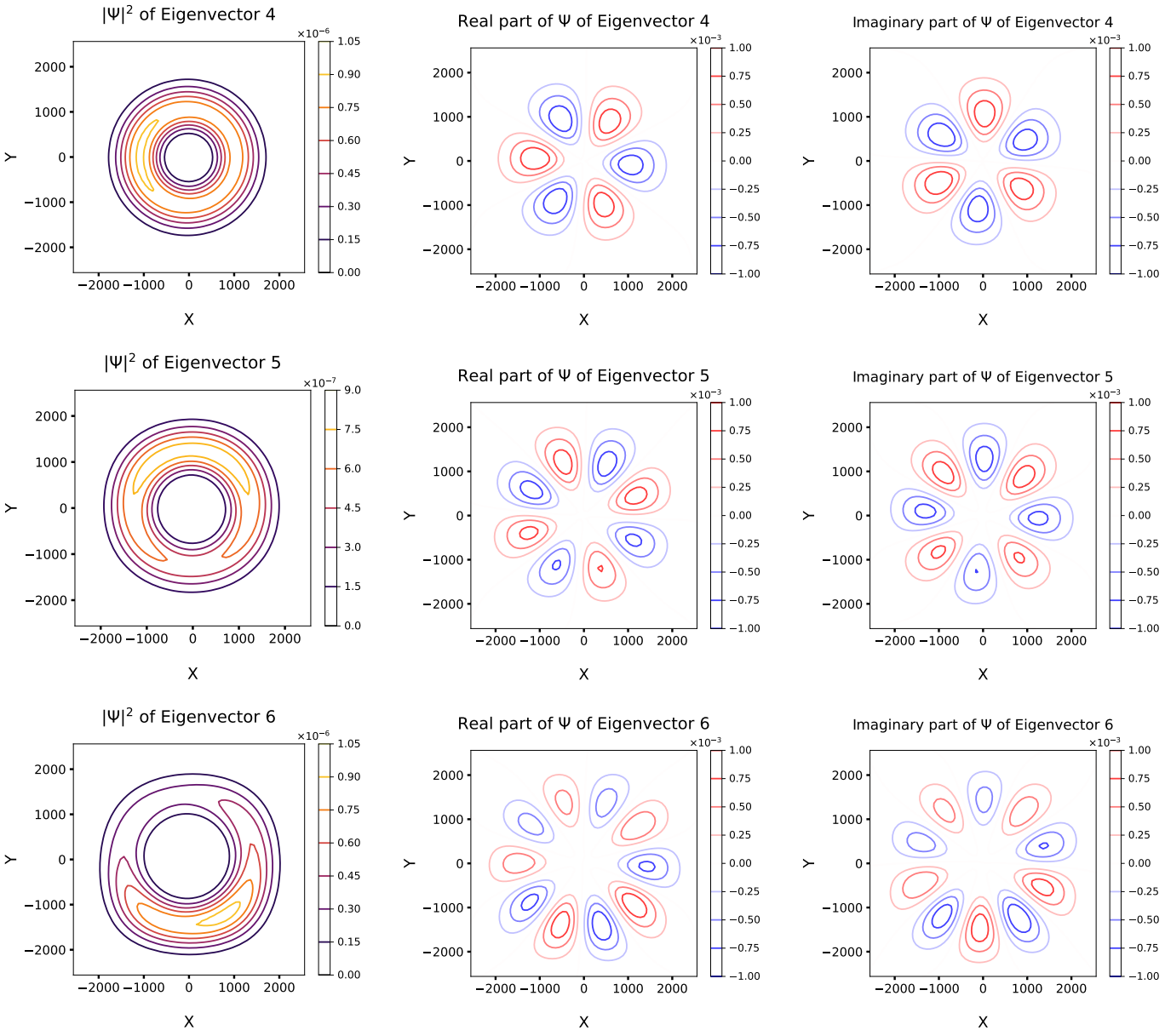

Figure 26: The probability density, real and imaginary contour plots of the 4th, 5th and 6th numerically obtained eigenfunctions obtained using ITP for magnetic field strength B = 5 T.

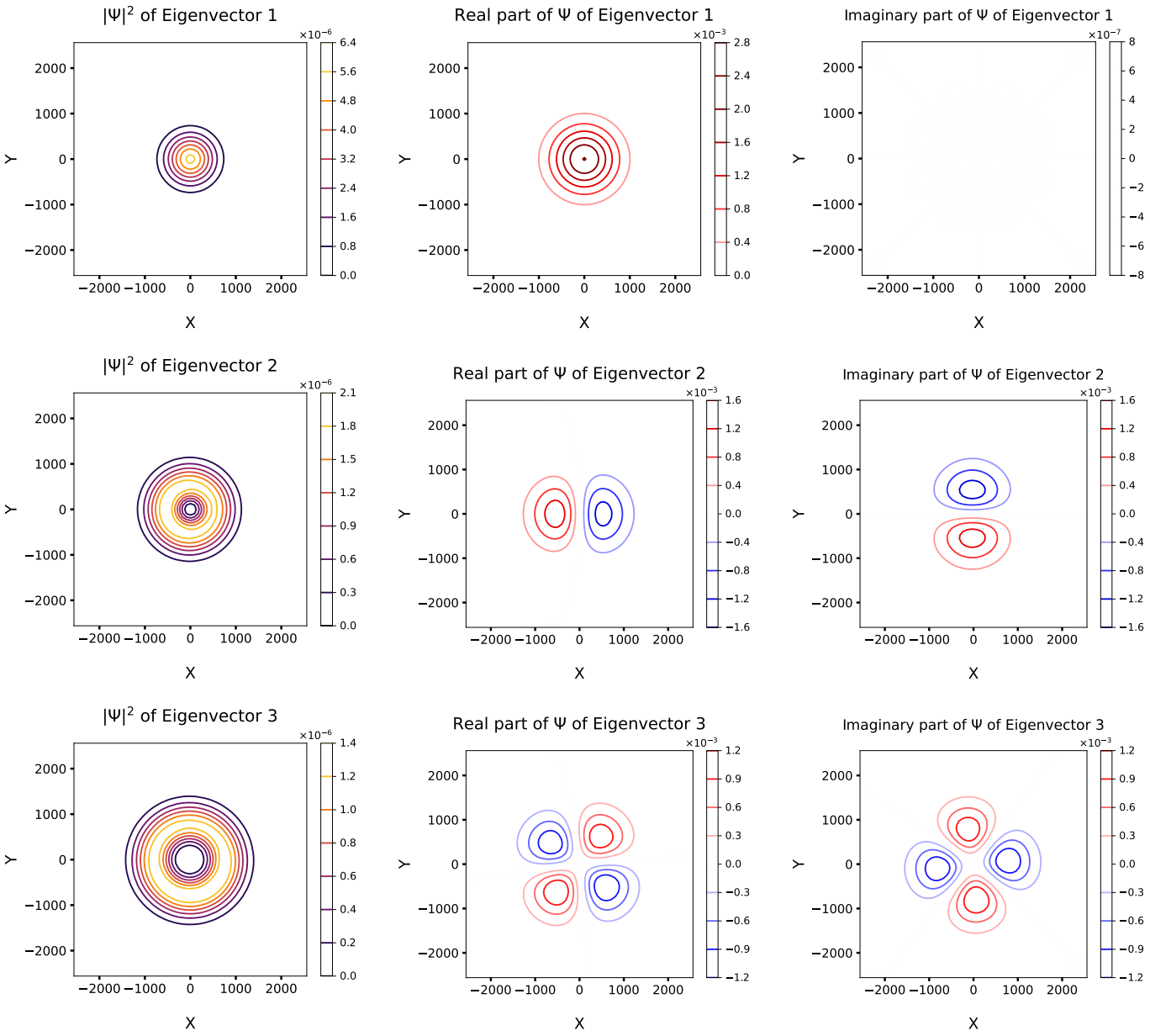

Figure 27: The probability density, real and imaginary contour plots of the 1st, 2nd and 3rd numerically obtained eigenfunctions obtained using ITP for magnetic field strength B = 6 T.

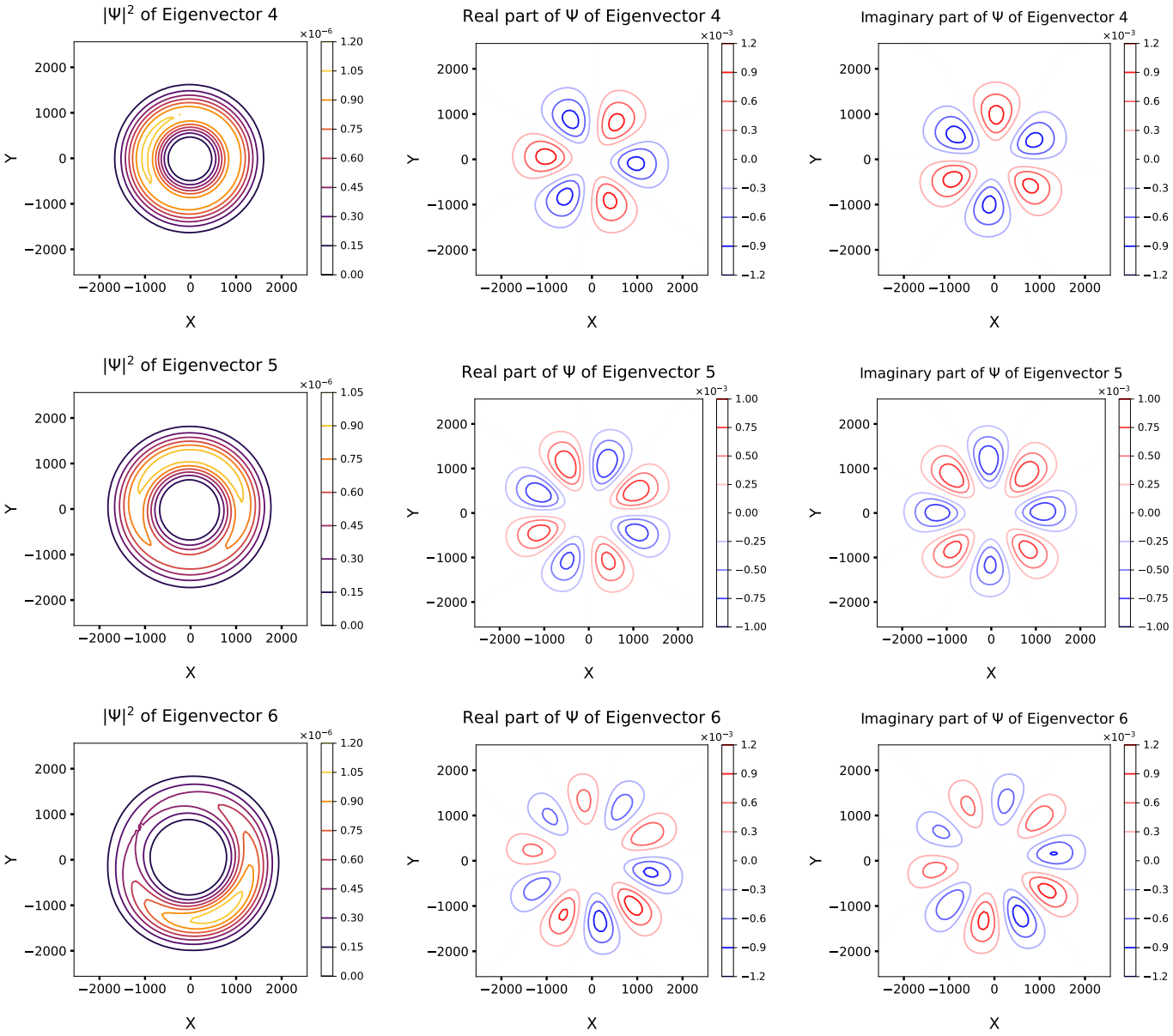

Figure 28: The probability density, real and imaginary contour plots of the 4th, 5th and 6th numerically obtained eigenfunctions obtained using ITP for magnetic field strength B = 6 T.

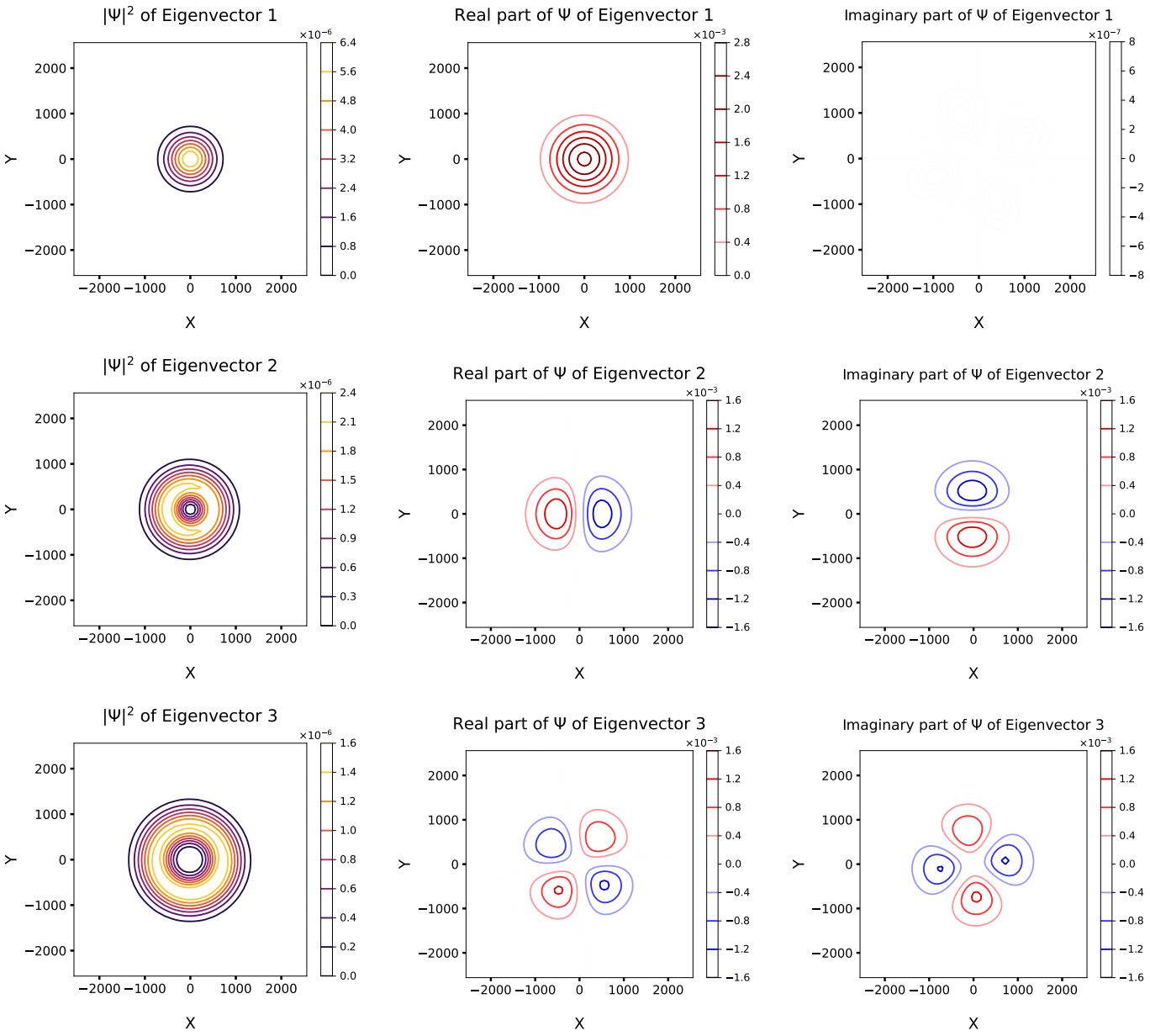

Figure 29: The probability density, real and imaginary contour plots of the 1st, 2nd and 3rd numerically obtained eigenfunctions obtained using ITP for magnetic field strength B = 7 T.

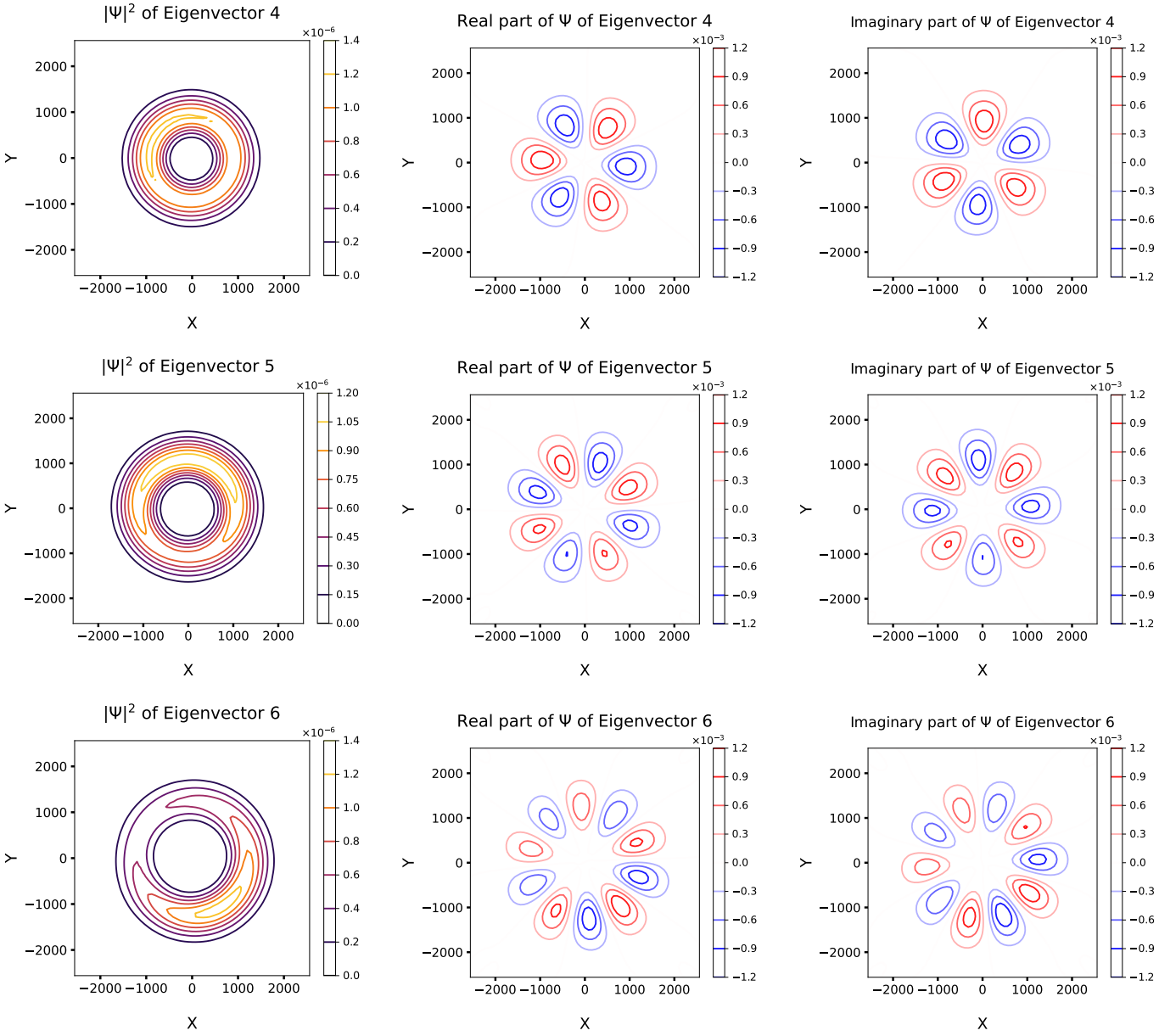

Figure 30: The probability density, real and imaginary contour plots of the 4th, 5th and 6th numerically obtained eigenfunctions obtained using ITP for magnetic field strength B = 7 T.

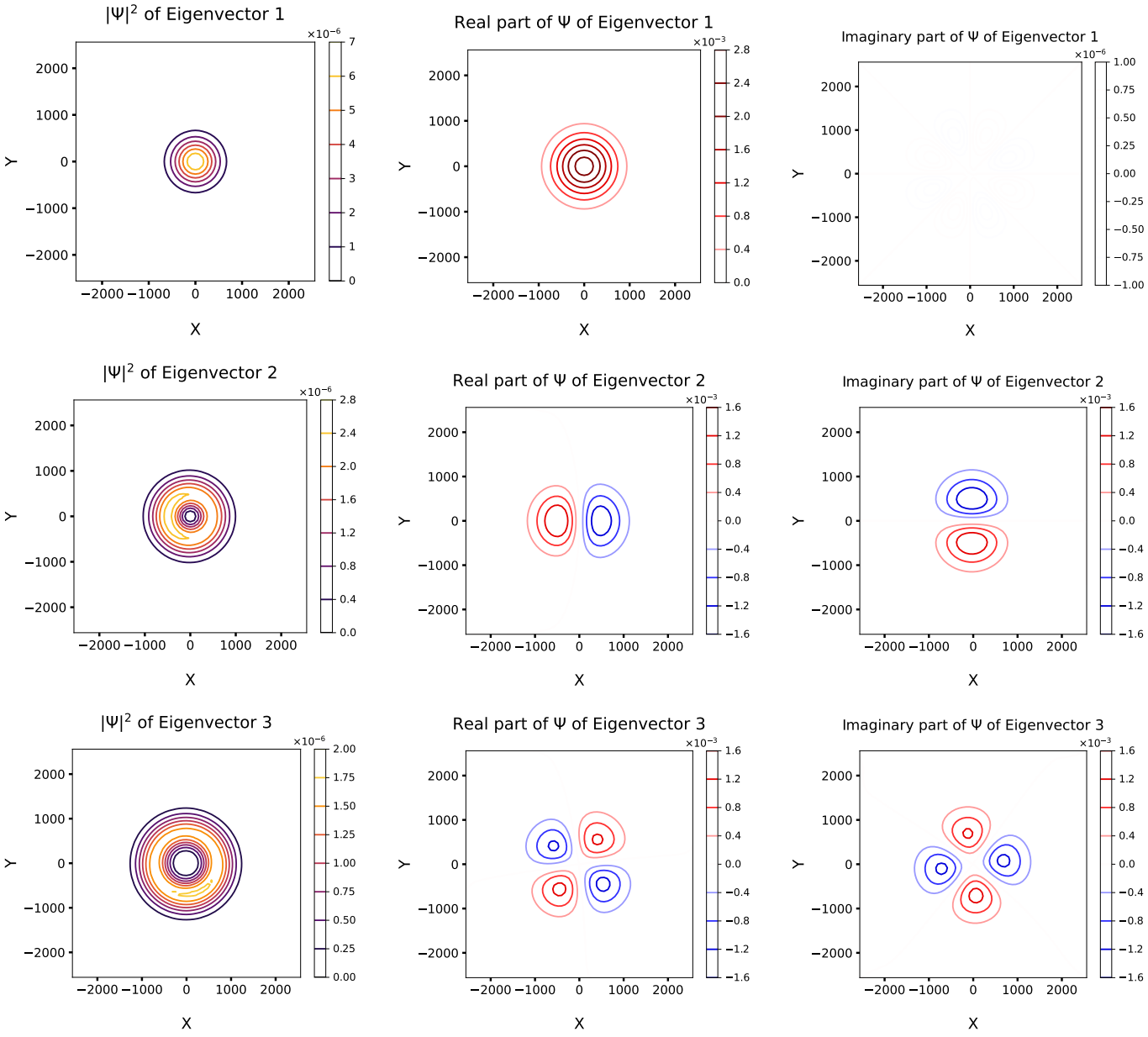

Figure 31: The probability density, real and imaginary contour plots of the 1st, 2nd and 3rd numerically obtained eigenfunctions obtained using ITP for magnetic field strength B = 8 T.

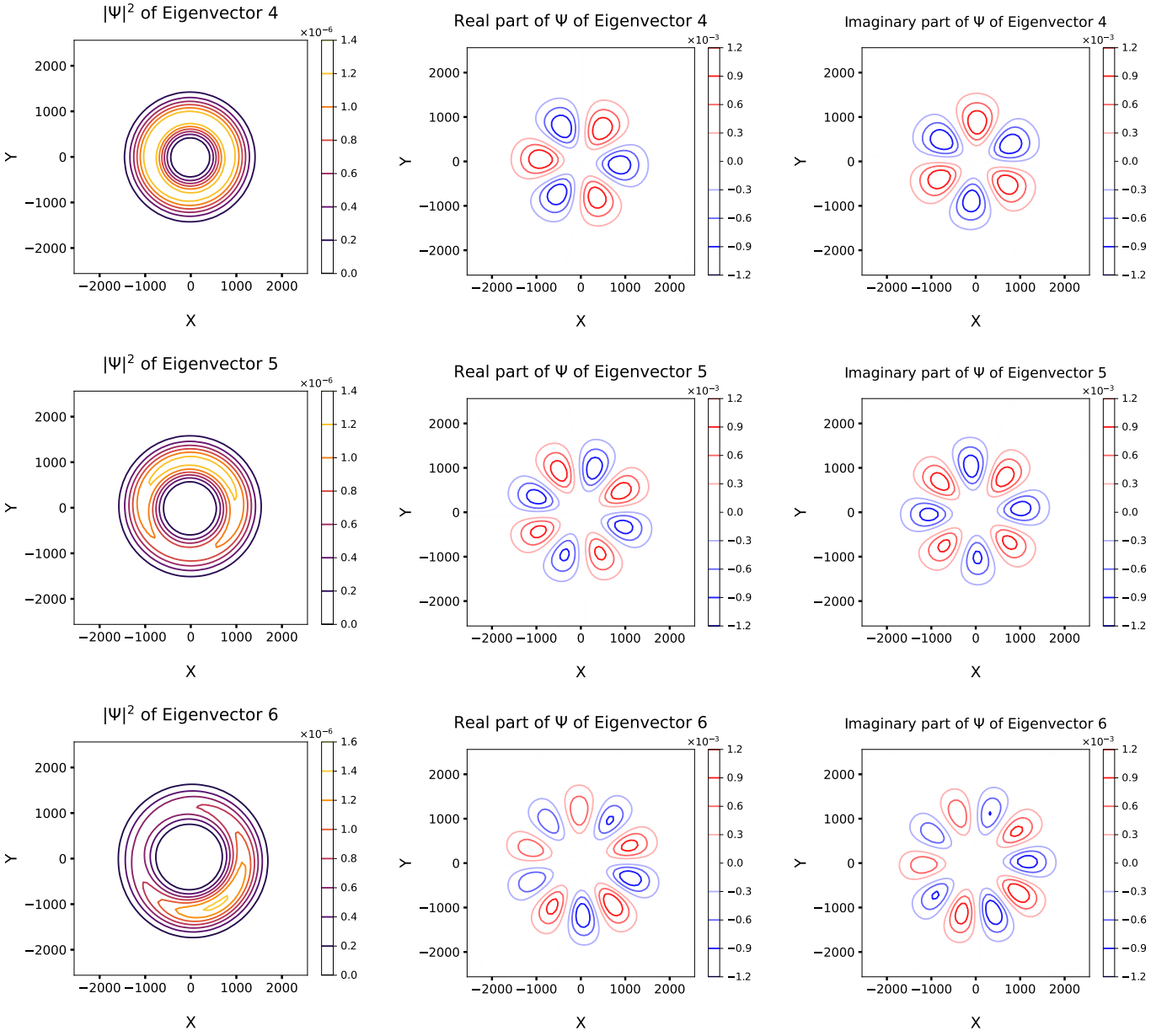

Figure 32: The probability density, real and imaginary contour plots of the 4th, 5th and 6th numerically obtained eigenfunctions obtained using ITP for magnetic field strength B = 8 T.

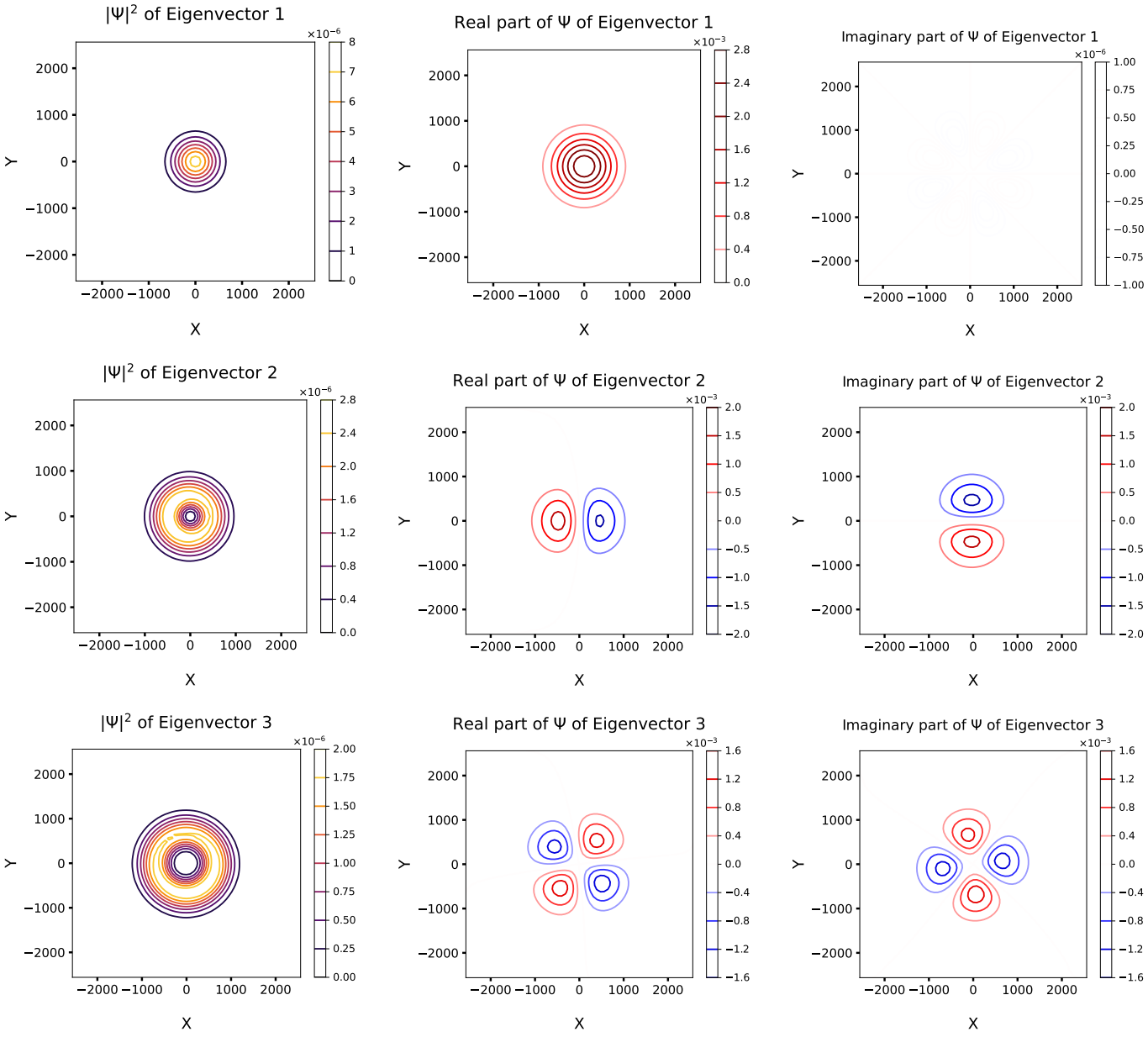

Figure 33: The probability density, real and imaginary contour plots of the 1st, 2nd and 3rd numerically obtained eigenfunctions obtained using ITP for magnetic field strength B = 9 T.

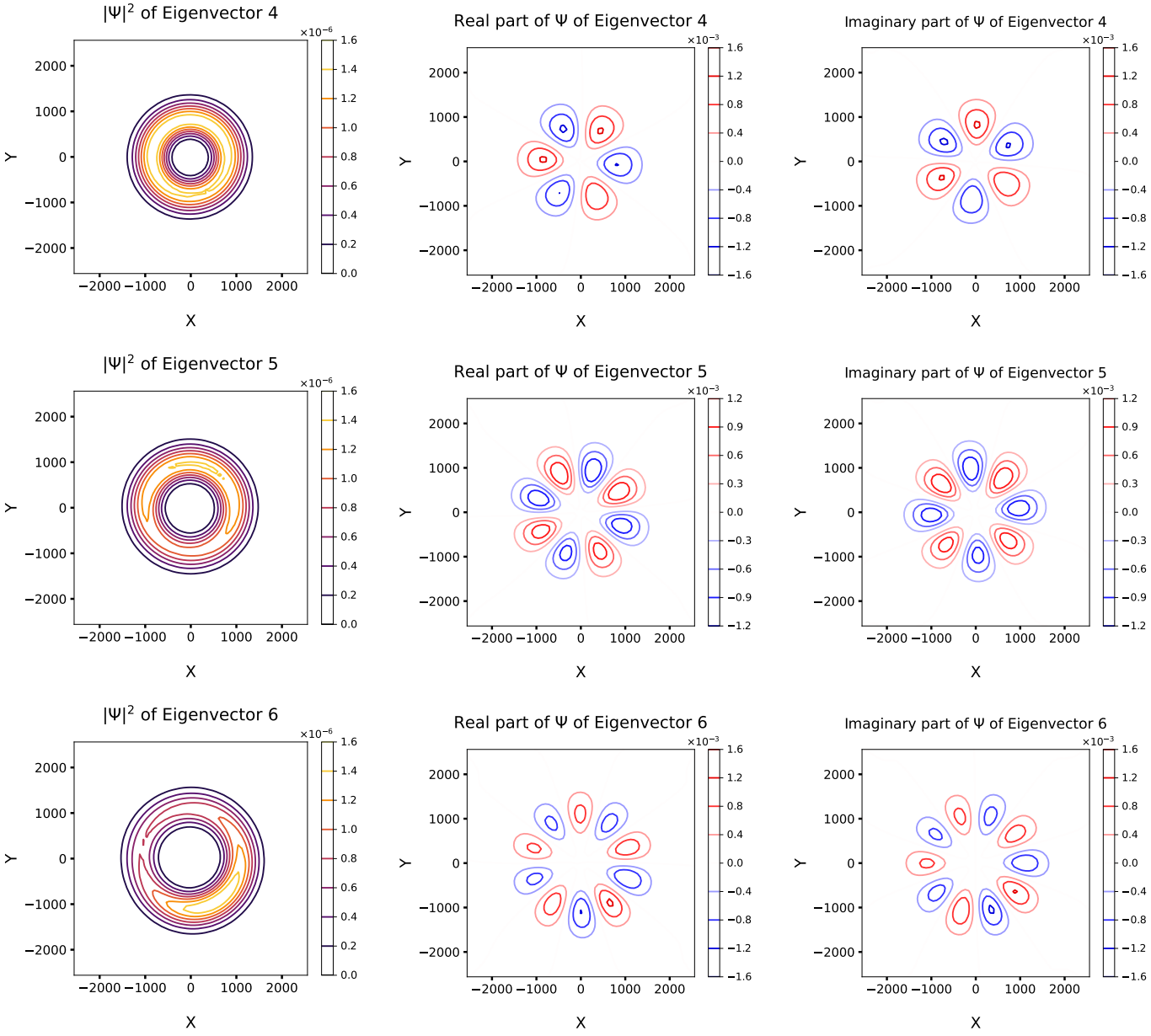

Figure 34: The probability density, real and imaginary contour plots of the 4th, 5th and 6th numerically obtained eigenfunctions obtained using ITP for magnetic field strength B = 9 T.

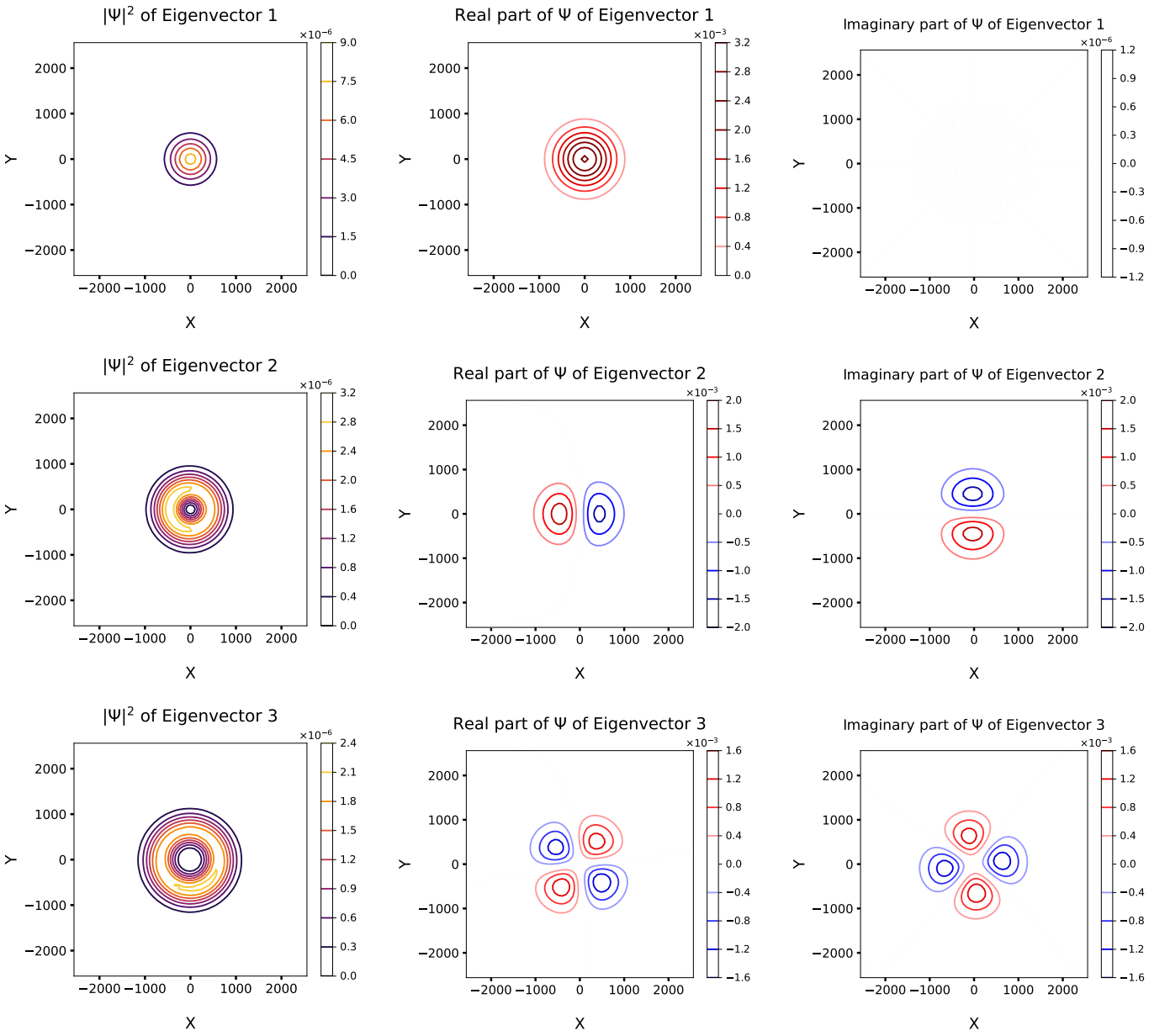

Figure 35: The probability density, real and imaginary contour plots of the 1st, 2nd and 3rd numerically obtained eigenfunctions obtained using ITP for magnetic field strength B = 10 T.

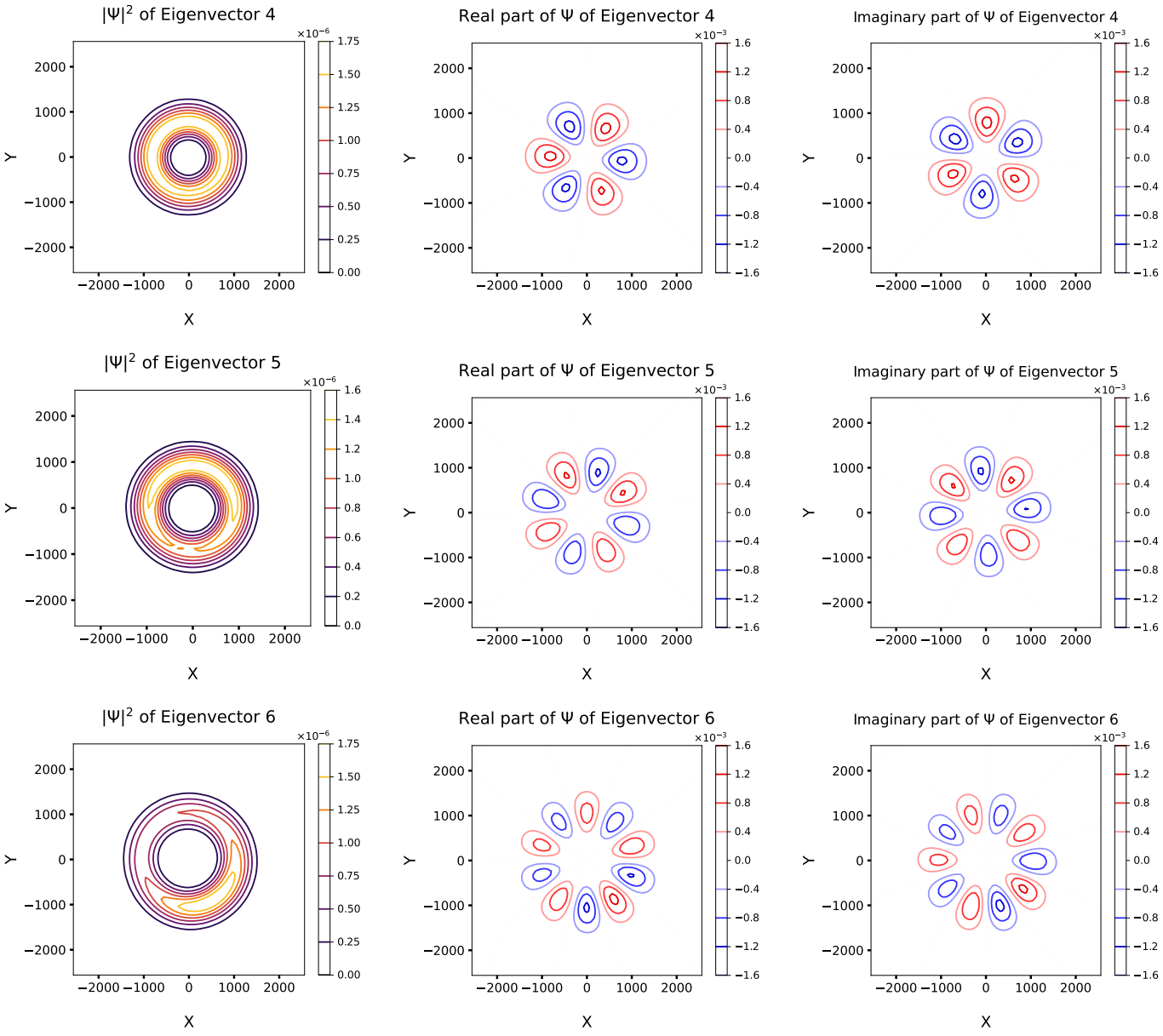

Figure 36: The probability density, real and imaginary contour plots of the 4th, 5th and 6th numerically obtained eigenfunctions obtained using ITP for magnetic field strength B = 10 T.